Mff is an essential factor for mitochondrial recruitment of Drp1 during mitochondrial fission in mammalian cells

Hidenori Otera,[1] Chunxin Wang,[2] Megan M. Cleland,[2] Kiyoko Setoguchi,[1] Sadaki Yokota,[3] Richard J. Youle,[2] and Katsuyoshi Mihara[1]

[1]Department of Molecular Biology, Graduate School of Medical Science, Kyushu University, Fukuoka 812-8582, Japan
[2]Biochemistry Section, Surgical Neurology Branch, National Institute of Neurological Disorders and Stroke, National Institutes of Health, Bethesda, MD 20892
[3]Pharmaceutical Sciences, Nagasaki International University, Sasebo 859-3298, Japan

The cytoplasmic dynamin-related guanosine triphosphatase Drp1 is recruited to mitochondria and mediates mitochondrial fission. Although the mitochondrial outer membrane (MOM) protein Fis1 is thought to be a Drp1 receptor, this has not been confirmed. To analyze the mechanism of Drp1 recruitment, we manipulated the expression of mitochondrial fission and fusion proteins and demonstrated that (a) mitochondrial fission factor (Mff) knockdown released the Drp1 foci from the MOM accompanied by network extension, whereas Mff overexpression stimulated mitochondrial recruitment of Drp1 accompanied by mitochondrial fission; (b) Mff-dependent mitochondrial fission proceeded independent of Fis1; (c) a Mff mutant with the plasma membrane–targeted CAAX motif directed Drp1 to the target membrane; (d) Mff and Drp1 physically interacted in vitro and in vivo; (e) exogenous stimuli–induced mitochondrial fission and apoptosis were compromised by knockdown of Drp1 and Mff but not Fis1; and (f) conditional knockout of Fis1 in colon carcinoma cells revealed that it is dispensable for mitochondrial fission. Thus, Mff functions as an essential factor in mitochondrial recruitment of Drp1.

Introduction

Mitochondrial morphology is dynamically changed by continuous fission and fusion to form small units or interconnected mitochondrial networks, and this dynamic morphology is essential for normal mitochondrial and cellular functions (Karbowski and Youle, 2003; Okamoto and Shaw, 2005; Chan, 2006; McBride et al., 2006; Cerveny et al., 2007b; Hoppins et al., 2007; Benard and Karbowski, 2009). These morphological changes are closely associated with apoptosis: apoptotic stimuli trigger extensive mitochondrial fission accompanied by cristae disorganization, permeabilization of the mitochondrial outer membrane (MOM), and release of apoptosis regulatory proteins, including cytochrome *c* (Scorrano et al., 2002; Frezza et al., 2006). High molecular weight GTPases are key regulators of these morphological dynamics. In mammals, mitofusin proteins (Mfn1 and Mfn2) of MOM and the inner membrane protein Opa1 are essential for mitochondrial fusion (Alexander et al., 2000; Delettre et al., 2000; Santel and Fuller, 2001). Opa1 is also involved in cristae remodeling (Olichon et al., 2003). Cristae are thought to trap large pools of cytochrome *c*, and down-regulation of Opa1 may lead to the opening of cristae junctions and mobilization of cytochrome *c*, which is released into the cytosol by a Bax/Bak-dependent mechanism. Another dynamin-related GTPase, Drp1 (Dnm1 in yeast), is involved in mitochondrial fission. Dnm1, localizing in the cytosol as self-assembled punctate structures, is recruited to the MOM receptor Fis1 through the adaptor protein Mdv1 (or its paralogue Caf4), self-assembles into helical structures, and drives membrane scission in a GTP-dependent manner (Okamoto and Shaw, 2005; Cerveny et al., 2007b; Hoppins et al., 2007).

Correspondence to Katsuyoshi Mihara: mihara@cell.med.kyushu-u.ac.jp

Abbreviations used in this paper: CCCP, carbonyl cyanide m-chlorophenylhydrozone; CKO, conditional KO; DSP, dithiobis (succinimidyl propionate); FRT, flippase recognition target; IRES, internal ribosome entry site; KO, knockout; MEF, mouse embryonic fibroblast; Mff, mitochondrial fission factor; MOM, mitochondrial outer membrane; Neo, Neomycin; ROI, region of interest; shRNA, short hairpin RNA; TMD, transmembrane domain; WT, wild type.

The Rockefeller University Press $30.00
J. Cell Biol. Vol. 191 No. 6 1141–1158
www.jcb.org/cgi/doi/10.1083/jcb.201007152

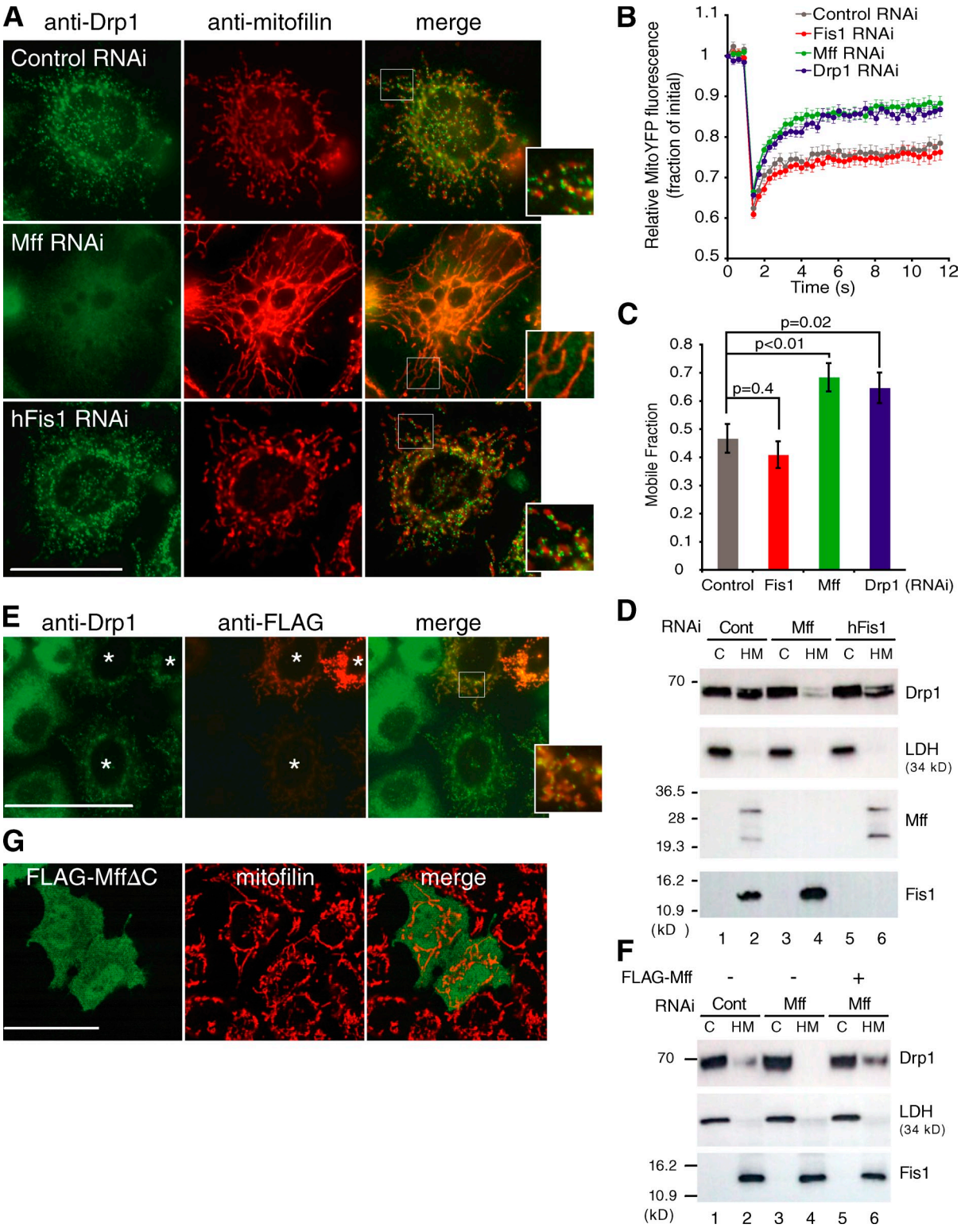

Figure 1. ***Mff* siRNA compromises mitochondrial localization of Drp1.** (A) Control, *Mff*, or *Fis1* RNAi HeLa cells were analyzed by immunofluorescence microscopy using anti-Drp1 antibody (green) and antimitofilin antibodies (red). Magnified images are shown in insets. (B and C) Mitochondrial network connectivity in either control, *Fis1*, *Mff*, or *Drp1* RNAi HeLa cells transfected with mito-YFP. In brief, a 2.1-µm circle containing multiple mitochondria was photobleached and monitored for recovery (Fig. S2). The normalized and photobleach corrected curves (B) or mobile fractions (C) represent the mean ± SEM of 60 individual FRAP curves from two independent experiments (30 FRAP curves per experiment). The results were analyzed by the Student's *t* test, and p-values are noted on the figure. (D) HeLa cells transfected with the indicated siRNAs were fractionated into cytosol (C) and heavy membrane (HM) fractions, which were analyzed by Western blotting using the indicated antibodies (cytosol/heavy membrane = 1:5 in volume equivalents). Five times the volume equivalent of heavy membrane fraction versus cytosol fraction was loaded to show the difference on mitochondrial recruitment of Drp1 in control (Cont) and *Mff* RNAi cells. Lactate dehydrogenase (LDH) is a cytosolic marker. (E) *Mff* RNAi cells were transfected with FLAG-Mff and subjected to immunostaining with anti-Drp1 (green) and anti-FLAG (red) antibodies. Asterisks indicate FLAG-Mff–expressing cells. (F) HeLa cells subjected to the indicated

The fundamental molecular mechanisms of mitochondrial fission seem to be conserved across species because the mammalian homologues of yeast Fis1 (hFis1 for human homologues) and Drp1 (Smirnova et al., 2001; James et al., 2003; Yoon et al., 2003; Stojanovski et al., 2004) have been identified, whereas homologues for Mdv1 and Caf4 have not. Drp1 localizes throughout the cytosol, and a minor fraction of Drp1 localizes to the mitochondrial foci representing future fission sites (Smirnova et al., 2001; Benard and Karbowski, 2009). In mammals, the mechanism of the mitochondrial recruitment of Drp1 by MOM proteins remains unclear. As in yeast, exogenous expression of *hFis1* induces mitochondrial fragmentation, and down-regulation of *hFis1* induces a perinuclear accumulation of elongated mitochondria. Furthermore, Drp1 and hFis1 coimmunoprecipitate after cross-linking in vitro, suggesting that mitochondrial fission mechanisms are somewhat conserved throughout eukaryotes (Yoon et al., 2003). Mitochondria undergo extensive fragmentation early during apoptosis, and Drp1 is essential for the normal progression of apoptosis (Youle and Karbowski, 2005; Parone and Martinou, 2006; Arnoult 2007; Suen et al., 2008; Ishihara et al., 2009). In this context, *hFis1* overexpression induces Drp1-dependent mitochondrial fission and apoptosis, and, conversely, *hFis1* knockdown inhibits the progression of apoptosis (Lee et al., 2004). However, there are conflicting observations: hFis1 localizes throughout the MOM in contrast to the punctate localization of Drp1, and mitochondrial recruitment of Drp1 is not affected by *hFis1* knockdown (Lee et al., 2004; Stojanovski et al., 2004; Wasiak et al., 2007). Similarly, neither mitochondria-associated Drp1 nor mitochondrial fission is affected by *hFis1* overexpression (Suzuki et al., 2003). These contradictory observations on hFis1 may suggest that, although Fis1 is required for the mitochondrial fission, the Fis1 level is not a limiting factor in the mitochondrial fission process and mitochondrial recruitment of Drp1 is regulated by other elements.

In addition to Fis1, MOM-anchored proteins ganglioside-induced differentiation–associated protein 1 (GDAP1; Niemann et al., 2005) and RING (really interesting new gene)-type E3-ubiquitin ligase March5/MITOL (Karbowski et al., 2007) are involved in mitochondrial fission. A recent study identified another tail-anchored MOM protein mitochondrial fission factor (Mff; Gandre-Babbe and van der Bliek, 2008). However, their specific roles in Drp1-dependent mitochondrial fission are not known.

Here, we study the requirement of mitochondrial proteins for mitochondrial targeting of Drp1 by manipulating the expression of mitochondrial fission and fusion proteins, including hFis1, Mff, March5/MITOL, GDAP1, and Opa1, and found that Mff clearly limited Drp1 function in mitochondrial fission and apoptosis. In contrast, these effects were not observed for the other proteins, including hFis1. In this context, Drp1 and Mff physically interacted both in vivo and in vitro. Furthermore, conditional knockout (KO; CKO) of hFis1 in human colon carcinoma cells revealed that hFis1 is dispensable for mitochondrial fission. We thus concluded that Mff, but not hFis1, is an essential factor for mitochondrial recruitment of Drp1 during mitochondrial fission in mammalian cells.

Results

Mff down-regulation inhibits mitochondrial recruitment of Drp1 and induces mitochondria elongation

We first examined the effect of *Mff* knockdown on mitochondrial localization of Drp1 and mitochondrial morphology using three independent pairs of oligonucleotides, two of which efficiently reduced endogenous levels of Mff (Fig. S1 A). *Mff* RNAi (#2; Mff depletion ∼94%) induced formation of closed mitochondrial networks similar to when the fission was inhibited by *Drp1* RNAi (Fig. 1 A and Fig. S1 C), confirming the findings of Gandre-Babbe and van der Bliek (2008). Unexpectedly, eight independent oligonucleotide pairs for *hFis1* (four siRNAs and four short hairpin RNAs [shRNAs]), including one previously reported to be effective (Koch et al., 2005), significantly reduced the hFis1 levels in HeLa cells (hFis1 depletion ∼95%; Fig. S3 A and see Fig. 9 C) but resulted in only weak or no mitochondrial morphology changes (note that some siRNA and shRNA induced an increase of the cell volume, which apparently resulted in subtle mitochondrial morphology changes; Fig. 1 A; see Fig. 9, C and D; Fig. S1 C; and Fig. S3 B). The mitochondria in *Mff* RNAi cells had fewer free ends than those in *hFis1* RNAi or control cells (Fig. 1 A and Fig. S1 C). Many balloon- or bulblike structures were observed at the base of the mitochondrial tubules in *Drp1* and *Mff* RNAi cells but not in *hFis1* RNAi cells (Fig. S1 C). We concluded that *Mff* RNAi caused similar mitochondrial morphology changes as *Drp1* RNAi, and the effect was much stronger than those induced by *hFis1* RNAi. A quantitative FRAP assay that measures mitochondrial connectivity confirmed that *Mff* RNAi cells and *Drp1* RNAi cells had significantly faster recovery rates and higher mobile fractions of mitochondrial YFP (mito-YFP) fluorescence than *hFis1* RNAi and control RNAi cells (Fig. 1, B and C; and Fig. S2).

We then examined whether *Mff* RNAi affects the intracellular distribution of Drp1. In contrast to control RNAi cells, Drp1 foci on the mitochondria was clearly decreased and rather was dispersed throughout the cytoplasm in *Mff* RNAi cells (Fig. 1 A). In contrast, *hFis1* RNAi did not affect the mitochondrial localization of Drp1 as previously reported (Fig. 1 A). These results were confirmed by cell fractionation. Drp1 in mitochondrial fraction was significantly reduced in *Mff* RNAi cells but not in control and hFis1 RNAi cells (Fig. 1 D). Knockdown of other MOM proteins, including March5/MITOL, preprotein import receptors Tom20, Tom22, and Tom70, VDAC1 and 2, and GDAP1, did not affect the mitochondrial distribution of Drp1 (unpublished data).

The *Mff* gene encodes at least nine different splice variants, although their functional difference is not known (Gandre-Babbe

manipulations were fractionated and analyzed as in D. Cytosol/heavy membrane = 1:3 in volume equivalents. (G) FLAG-Mff mutant lacking a TMD (MffΔC) was expressed in HeLa cells. After incubation for 24 h, the cells were fixed and immunostained with anti-FLAG antibody (green) and antimitofilin antibodies (red). Bars, 20 µm.

and van der Bliek, 2008). Hereafter, we analyze variant 8 dominantly expressed in HeLa cells (Fig. S1 B). Expression of FLAG-Mff completely restored mitochondrial recruitment of Drp1 in Mff RNAi cells (variant 6 was equally effective; Fig. 1 E, asterisks; and Fig. S1 D). These results were further confirmed by cell fractionation (Fig. 1 F), indicating that Mff functions in mitochondrial fission by regulating the mitochondrial recruitment step of Drp1.

Exogenous expression of Mff induces extensive mitochondrial fission

We next investigated whether expression of Mff induces mitochondrial fission. A stable HeLa cell line expressing the mitochondrial matrix–targeted precursor Su9-DsRed was transfected with the plasmid pMff–*internal ribosome entry site* (*IRES*)–GFP-NLS, which directs coexpression of untagged Mff and a nuclear-targeted GFP (GFP-NLS) under a single promoter. More than 80% of the cells had extensively fragmented mitochondria irrespective of the Mff expression level (Fig. 2, A and B). The same results were obtained when Tom22 was analyzed as the MOM marker (Fig. 2 C), indicating that Mff promotes mitochondrial fission. However, no such mitochondrial fragmentation was detected in cells expressing the Mff mutant lacking the transmembrane domain (TMD) and dispersed to the cytoplasm (MffΔC; Fig. 1 G), indicating that Mff functioning on the correct membrane is a prerequisite for mitochondrial fission. In contrast to our findings, it was previously reported that exogenously expressed Mff (variant 8) does not stimulate mitochondrial fission (Gandre-Babbe and van der Bliek, 2008). We have no adequate explanation for this discrepancy.

Because mammalian Fis1 was previously shown to induce mitochondrial fission (James et al., 2003; Yoon et al., 2003), we reevaluated the effect of hFis1 in our assay system and compared it with Mff activity. Expression of hFis1 collapsed the mitochondrial networks with much weaker morphological changes than those induced by Mff, and high hFis1 expression induced perinuclear aggregation of vesiculated mitochondria (Fig. 2, A–C). Notably, the hFis1-induced fragmented mitochondria were significantly larger than the Mff-induced ones. Together, these observations indicated that Mff has a stronger effect on mitochondrial fission than hFis1.

Mff localizes in puncta on mitochondria

Immunofluorescence microscopy revealed that Mff is localized mostly in puncta on mitochondria, and the disappearance of the puncta in Mff RNAi cells was accompanied by the extension of mitochondrial tubular network structures (Fig. 2 D), confirming that those structures were Mff related. Interestingly, these structures were detected on the extended tubular networks in *Drp1* RNAi cells but were not affected by *hFis1* RNAi or *Drp1/hFis1* double RNAi (unpublished data for *Drp1/hFis1* RNAi), suggesting that Mff is present as preassembled structures on the MOM irrespective of Drp1 or hFis1 expression. Notably, double immunofluorescence staining and a line scan plot of Mff and Drp1 revealed that they were mostly colocalized in foci on the MOM (Fig. 2, E and F).

Mff interacts with Drp1 on the MOM

To test whether Mff directly recruits Drp1 to the mitochondrial foci, we established a HeLa cell line overexpressing N-terminally FLAG-tagged Drp1. In this cell line, the vast majority of FLAG-Drp1 was localized in the cytoplasm but rarely detected on mitochondria by immunofluorescence microscopy (Fig. 3 A, a). The cells were then transfected with pMff-*IRES*-GFP-NLS to simultaneously express Mff and nuclear-targeted GFP. More than 94% of the GFP-overexpressing cells exhibited the Drp1-positive and dotlike structures that were colocalized with Mff on the mitochondria (Fig. 3, A [c] and B). In contrast, no such changes were detected in the cells transfected with the phFis1-*IRES*-GFP-NLS plasmid (Fig. 3 A, b), although *hFis1* overexpression induced perinuclear accumulation of fragmented mitochondria (Fig. 2, A [f] and C). Importantly, Mff-dependent Drp1 recruitment was observed even in *hFis1* RNAi cells (Fig. 3 A, d), indicating that hFis1 is dispensable for the function of Mff in the mitochondrial recruitment of Drp1.

Next, we generated an Mff mutant in which the TMD of Mff was replaced with the secretory membrane–targeted CAAX motif (Robert et al., 2002) and expressed in the Mff-depleted HeLa cells. Mff-CAAX was localized to the plasma membrane, and endogenous Drp1 was colocalized with Mff-CAAX (Fig. 3 C), whereas it was diffusely localized throughout the cytoplasm in the cells not expressing Mff-CAAX (Fig. 3 C, asterisks), thus revealing an interaction of Mff and Drp1 in vivo.

To further confirm the interaction, we performed a coimmunoprecipitation assay. FLAG-Mff was coexpressed with HA-Drp1 in HeLa cells. Without cross-linking, Drp1 did not coprecipitate with FLAG-Mff, suggesting that the interaction between Mff and Drp1 is transient or unstable (unpublished data). Therefore, the cells were treated with the thiol-cleavable cross-linker dithiobis (succinimidyl propionate) (DSP) before membrane solubilization with either SDS (stringent condition) or digitonin (mild condition). DSP treatment did not change the subcellular localization pattern of Drp1 (unpublished data). Under the stringent condition, HA-Drp1 coimmunoprecipitated with FLAG-Mff but not with FLAG-hFis1 (Fig. 3 D). Interestingly, however, Drp1 and hFis1 coprecipitated under the mild condition. These results may suggest that Drp1 preferentially interacts with Mff to develop into oligomeric complexes, and hFis1 then interacts with the oligomerized Drp1; this later interaction might be detected only under the mild condition. As a control, neither the release of Drp1 foci from mitochondria nor mitochondrial accumulation of Drp1 was detected during the DSP treatment (unpublished data). Next, to directly address the interaction between Mff and Drp1, we performed immunoprecipitation in vitro using purified proteins and found that MffΔC coprecipitated with Drp1 after cross-linking (Fig. 3 E). In contrast to wild-type (WT) Drp1, Drp1 A395D mutant, identified from a human patient and with defects in higher order assembly and mitochondrial division (Waterham et al., 2007; Chang et al., 2010), failed to interact with MffΔC (Fig. 3 E). We found in this context that Drp1 A395D failed to be recruited to mitochondria in response to Mff overexpression (Fig. 3, F and G). Furthermore, coexpression of *Drp1 A395D* and *Mff* still stimulated mitochondrial network extension, exhibiting a dominant-negative effect similar to Drp1 K38A mutant (Fig. 3, H and I). Together, these

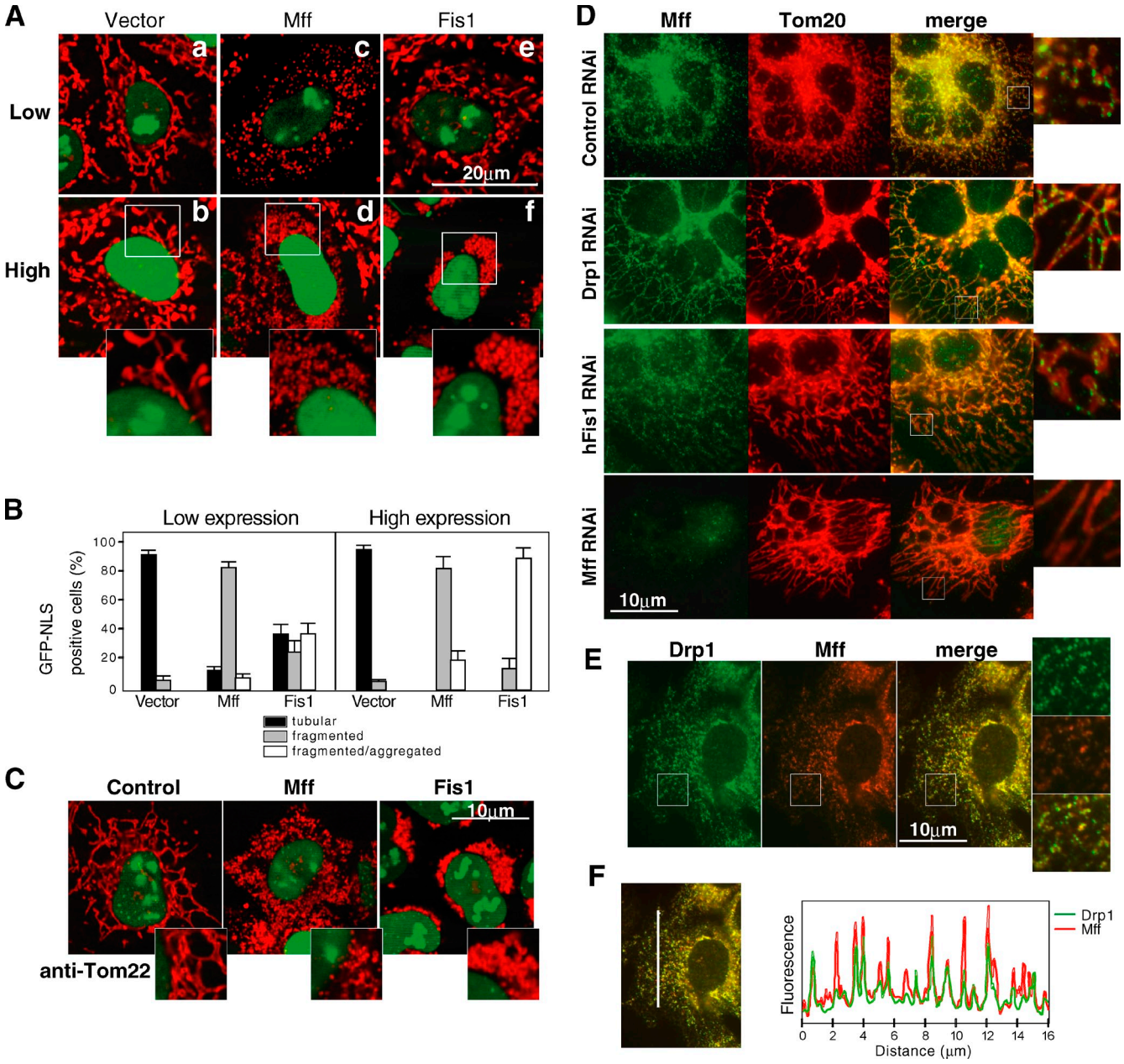

Figure 2. **Mff and Drp1 colocalize in puncta on mitochondria.** (A) *Mff* overexpression leads to mitochondrial fragmentation. HeLa cells stably expressing Su9-DsRed were transfected with pMff-*IRES*-GFP-NLS, phFis1-*IRES*-GFP-NLS, or empty vector and subjected to live imaging by confocal microscopy. Top and bottom images show the cells expressing low and high levels of nuclear GFP, respectively. Typical images are shown in insets at high magnification. (B) Percentages of cells with indicated mitochondrial morphologies in cells (n = 100) transfected with indicated plasmids at 24 h after transfection. Data were collected from three independent experiments and represent the mean ± SD. (C) HeLa cells manipulated as in A were immunostained with anti-Tom22 antibodies (red). The insets show magnified images of the mitochondrial regions. (D) Immunofluorescence microscopy of endogenous Mff in HeLa cells transfected with the indicated siRNA immunostained with anti-Mff (green) and anti-Tom20 (red). (E and F) HeLa cells were immunostained with anti-Drp1 (green) and anti-Mff (red) antibodies. (F) A line scan (shown in the vertical line) plot of relative fluorescence intensities of Mff and Drp1 in the indicated images (same as in E) was analyzed using AxioVision 4.7.1 software (Carl Zeiss, Inc.). The insets in D and E show magnified images of the squared regions.

results indicate that Mff plays a key role in recruiting Drp1 to the MOM to mediate mitochondrial fission.

The N-terminal cytosolic region of Mff is required for Drp1 recruitment to mitochondria

Mff is anchored to the MOM through the C-terminal TMD, extruding the bulk of the N-terminal portion containing two short amino acid repeats in the N-terminal half and a coiled-coil domain just upstream of the TMD into the cytosol (Gandre-Babbe and van der Bliek, 2008). To define the Mff region responsible for mitochondrial recruitment of Drp1, N-terminally truncated Mff constructs (Fig. 4 A) were expressed in *Mff* RNAi cells. Like full-length Mff, four truncated Mff constructs (MffΔ20, MffΔ50, MffΔ60, and MffΔ100) were localized to mitochondria (Fig. 4 B). However, mitochondrial recruitment of Drp1

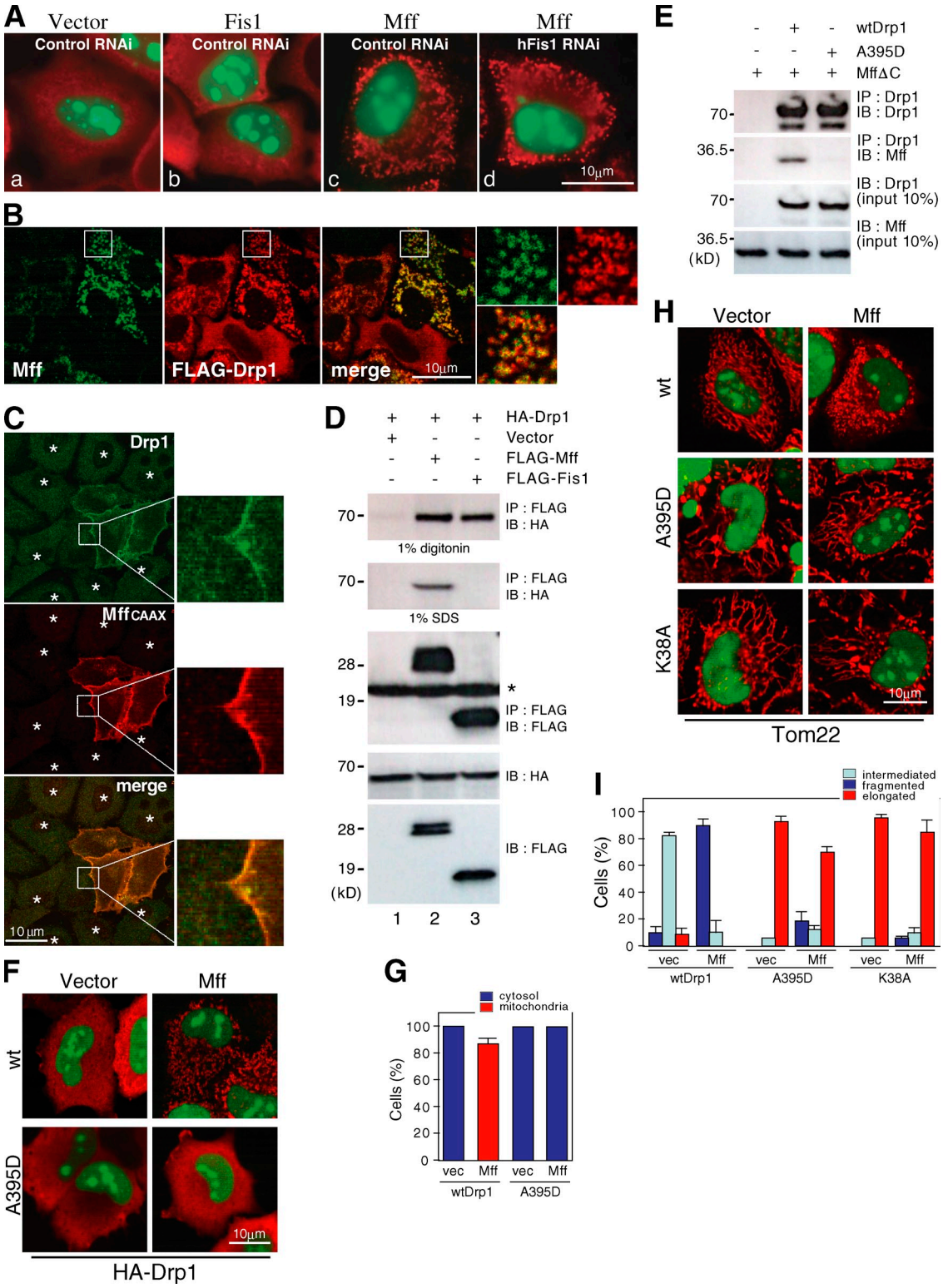

Figure 3. **Mff interacts with Drp1 both in vivo and in vitro.** (A) HeLa cells stably expressing FLAG-Drp1 were transfected with the indicated siRNA and further transfected with phFis1-*IRES*-GFP-NLS (b) and pMff-*IRES*-GFP-NLS (c and d). After 24 h, the cells were fixed and immunostained with anti-FLAG antibodies (red). (B) HeLa cells stably expressing FLAG-Drp1 were transfected with HA-Mff. After 24 h, the cells were immunostained with anti-HA antibodies (green) and anti-FLAG antibodies (red). High magnification images (insets) show colocalization of FLAG-Drp1 and HA-Mff. (C) HeLa cells were transfected with *Mff* siRNA and further transfected with FLAG-Mff-CAAX. The cells were immunostained with antibodies against Drp1 (green) and FLAG (red). Asterisks show FLAG-Mff-CAAX–nonexpressing cells. The insets show magnified images of the squared regions. (D) HeLa cells expressing the indicated proteins were treated with DSP, solubilized either with digitonin buffer (mild condition) or with SDS buffer (stringent condition), and subjected to immunoprecipitation (IP) using anti-FLAG antibody (see Materials and methods). Asterisk shows IgG light chain. IB, immunoblot. (E) Purified proteins were mixed in the indicated combinations and treated with 1 mM DSP. The reaction mixtures were solubilized with 1% Triton X-100 and subjected to immunoprecipitation with anti-Drp1 antibodies. See Materials and methods for details. (F) pMff-*IRES*-GFP-NLS was cotransfected with HA-WT-Drp1 or HA-Drp1-A395D into HeLa cells, and the

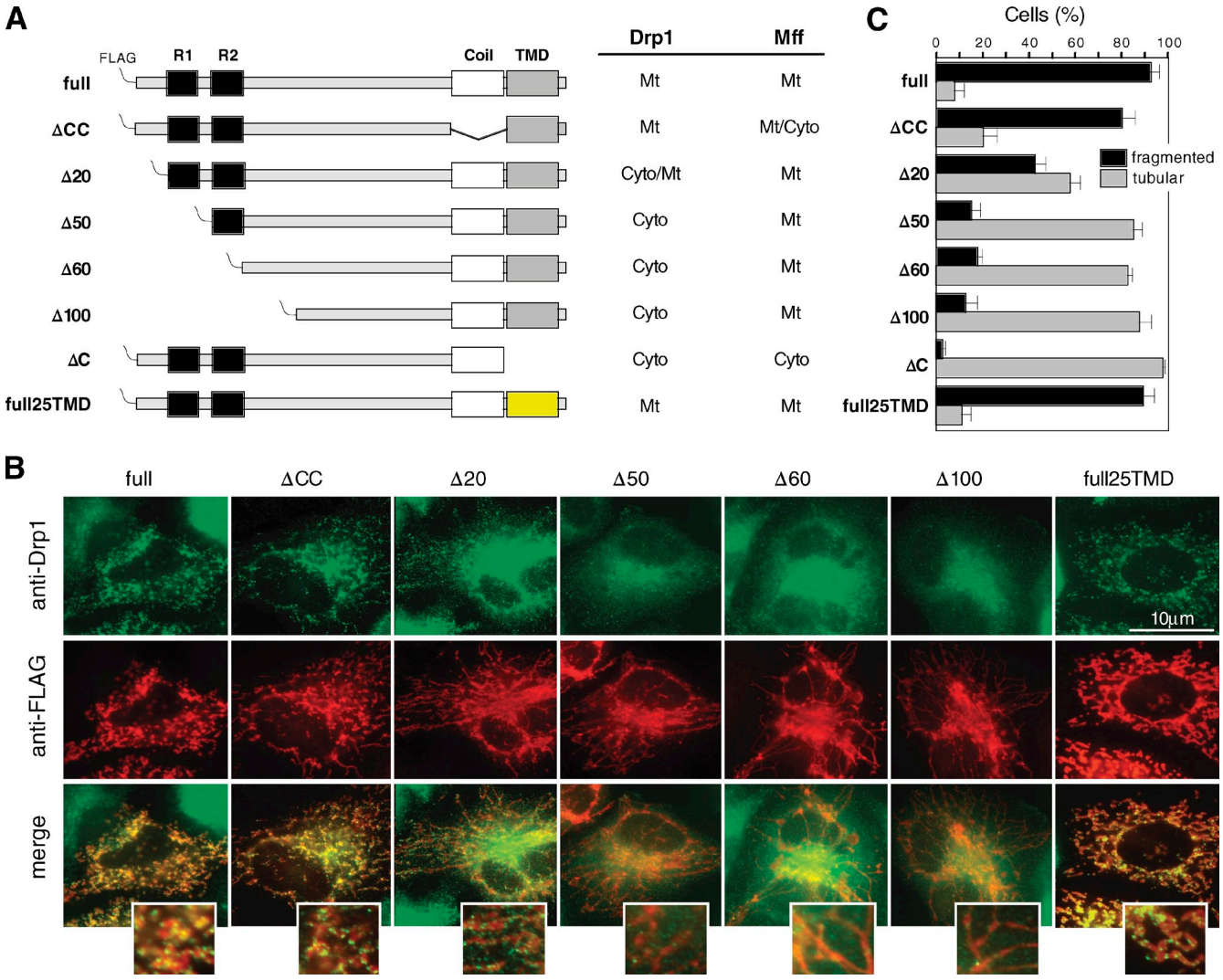

Figure 4. **N-terminal cytosolic region is required for the recruitment of Drp1 to mitochondria.** (A) Schematic representation of Mff deletion constructs, and summary of their expression effects on the recruitment and intracellular localization of Drp1 in *Mff* RNAi cells. Yellow box, TMD from Omp25. Mt, mitochondria. Cyto, cytoplasm. (B) Mff mutants were expressed in *Mff* RNAi cells and analyzed by immunofluorescence microscopy with anti-Drp1 (green) and anti-FLAG antibodies (red). The insets show magnified images of the mitochondrial regions. (C) Percentages of cells with the indicated mitochondrial morphologies in HeLa cells expressing various Mff deletion mutants as in B. 200 cells in each of three independent experiments were counted. Data represent mean ± SD.

was barely detectable for MffΔ50, MffΔ60, and MffΔ100. Partial deletion within the 1–20-residue segment (MffΔ20) slightly compromised the recruiting activity. In contrast, Drp1 recruitment was detected for the coiled-coil domain deletion mutant MffΔCC, whereas it was partly dispersed in the cytoplasm, suggesting that the coiled-coil domain is required for correct mitochondrial targeting of Mff. Together, these findings indicated that the N-terminal 50 residues containing one of the short amino acid repeats are essential for the Drp1 recruitment (Fig. 4 A). The TMD of Mff is not required for the Drp1 recruitment because the Mff mutant with the TMD of a MOM protein Omp25 (Setoguchi et al., 2006) had normal Drp1-recruiting activity (Fig. 4, A–C).

Knockdown of hFis1 does not interfere with Mff-dependent mitochondrial fission

To obtain definitive evidence for the Drp1-dependent function of Mff, the effect of FLAG-Mff expression on mitochondrial morphology was examined in *Drp1*$^{-/-}$ mouse embryonic fibroblast (MEF) cells (Ishihara et al., 2009). In WT cells, the expressed FLAG-Mff resulted in extensive mitochondrial fragmentation, whereas the extended mitochondrial network

cells were analyzed by immunofluorescence microscopy using anti-HA antibodies (red). Note that HA-WT-Drp1, but not HA-Drp1-G395A, was targeted to mitochondria in the Mff-expressing cells. (G) The cells (n = 200) for HA-WT-Drp1 and HA-Drp1-A395D with the cytosol- or mitochondria-localized pattern of Drp1 in A were quantified. vec, vector. (H) The cells treated as in F were analyzed by immunofluorescence microscopy using anti-Tom22. (I) Percentages of cells (n = 200) for HA-WT-Drp1, HA-Drp1-A395D, and HA-Drp1-K38A with the indicated mitochondrial morphology in H. Data were collected from three independent experiments and represent mean ± SD.

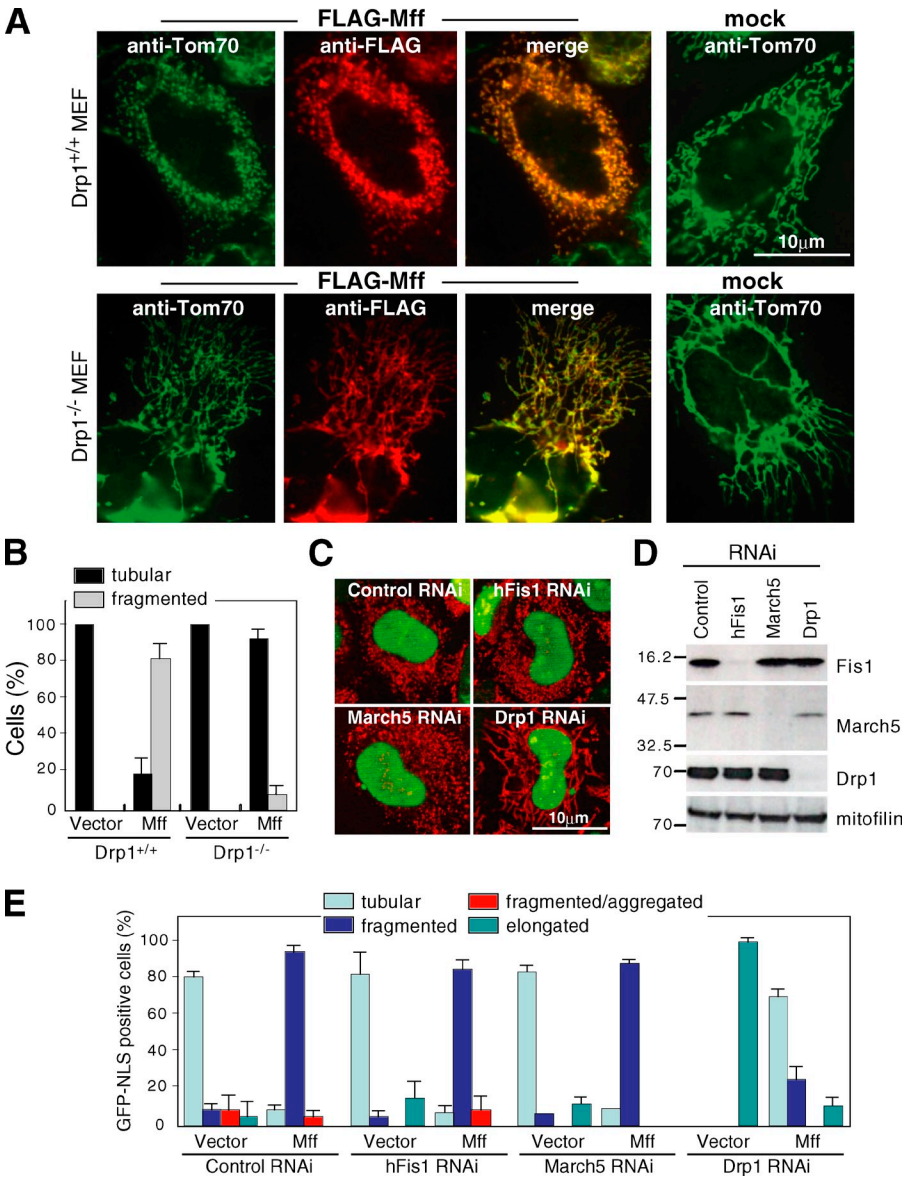

Figure 5. **Mff-induced mitochondrial fission depends on Drp1.** (A) FLAG-Mff was transfected in WT or *Drp1*$^{-/-}$ MEFs. After 36 h, the cells were fixed and immunostained with anti-Tom70 antibodies (green) and anti-FLAG antibodies (red). (B) Percentage of cells with tubular and fragmented mitochondria. Three distinct fields for each 100 cells were counted. Data represent mean ± SD. (C) HeLa cells stably expressing Su9-DsRed were transfected with the indicated siRNA and further transfected with pMff-*IRES*-GFP-NLS. Live images were obtained by confocal microscopy. (D) HeLa cells in C were subjected to immunoblot analysis using the indicated antibodies with mitofilin as a loading control. Molecular mass is given in kilodaltons. (E) Percentages of cells (n = 100) with the indicated mitochondrial morphologies in mock- and Mff-transfected cells at 24 h after transfection. Data were obtained from three independent experiments and represent mean ± SD.

structures in *Drp1*$^{-/-}$ MEFs were not affected by the expression of FLAG-Mff (Fig. 5, A and B). These results clearly demonstrated that Mff and Drp1 function together in the same mitochondrial fission pathway. We further found that the overexpressed *Mff* in *Fis1* RNAi cells induced mitochondrial fission to an extent comparable with that of the control RNAi cells (Fig. 5, C–E), confirming the results of the aforementioned Drp1 recruitment assay (Fig. 3 A, d) and suggesting that hFis1 cannot be the rate-limiting factor in the Mff-dependent mitochondrial fission.

Knockdown of Mff, but not hFis1, compromises carbonyl cyanide m-chlorophenylhydrozone (CCCP)–induced mitochondrial fission

We further evaluated the requirement of hFis1 and Mff in exogenous signal–triggered mitochondrial fission. Treatment of cultured cells with a protonophore, CCCP, leads to rapid mitochondrial fragmentation (Ishihara et al., 2006). A HeLa cell line stably expressing Su9-DsRed was transfected with siRNA for *Drp1*, *Mff*, or *hFis1* and incubated with CCCP (Fig. S3, D–F). Both *Drp1* RNAi and *Mff* RNAi strongly inhibited CCCP-induced mitochondrial fission. However, the inhibition was not observed in *hFis1* RNAi cells at any time point during incubation. Furthermore, simultaneous knockdown of *Mff* and *hFis1* did not have an additive phenotype, indicating that the function of Mff and hFis1 is not redundant.

Opa1 knockdown–induced mitochondrial fragmentation is suppressed by knockdown of either Drp1 or Mff but not hFis1

Opa1 knockdown causes extensive mitochondrial fragmentation and cristae disorganization with increased sensitivity to apoptotic stimuli (Olichon et al., 2003; Lee et al., 2004; Frezza et al., 2006). We took advantage of this response to further confirm the aforementioned results. *Mff/Opa1* double RNAi cells displayed elongated tubular mitochondria with bulb- or balloonlike structures similar to the phenotype in

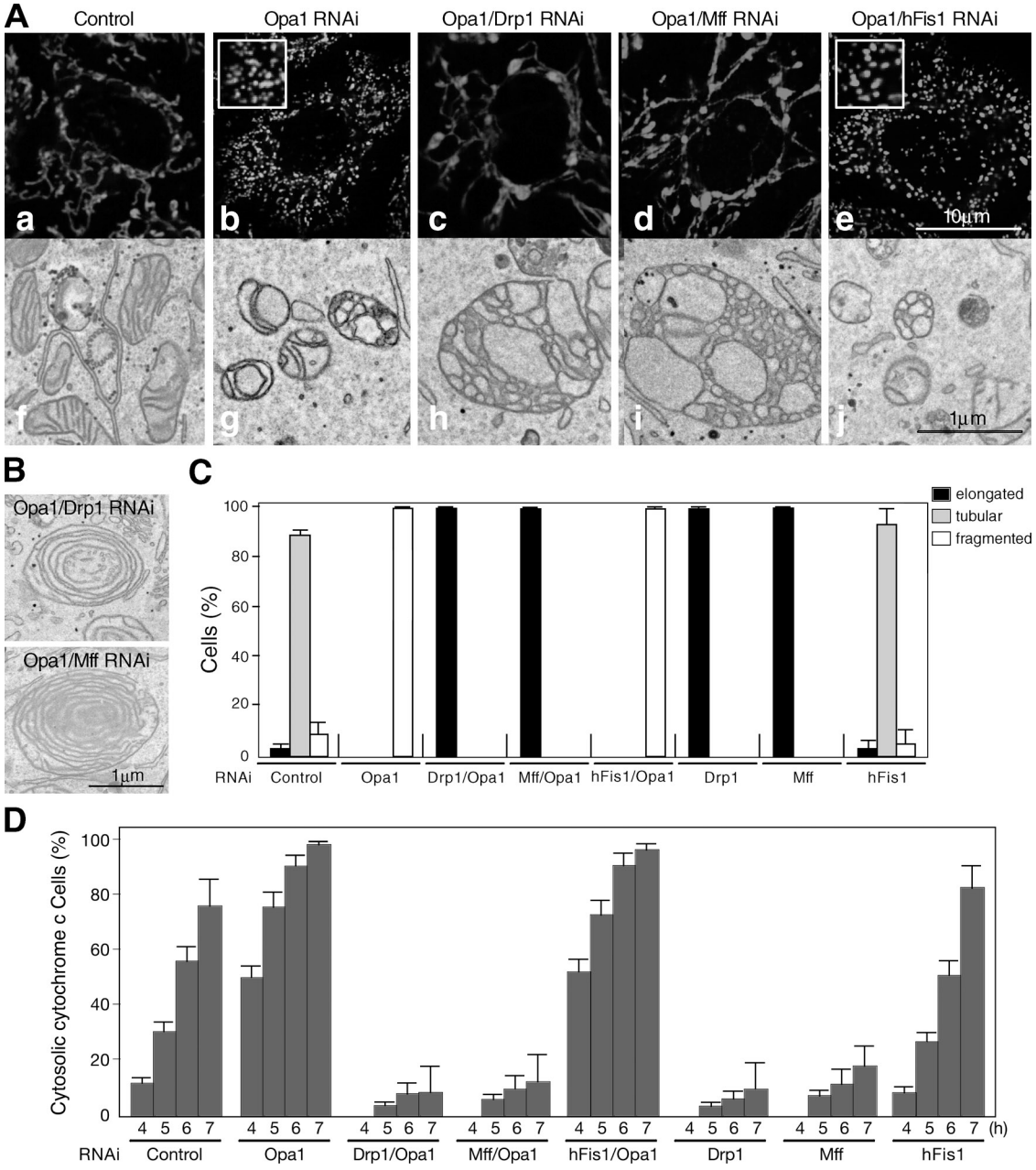

Figure 6. **Depletion of Mff, but not hFis1, blocks *Opa1* RNAi–induced extensive mitochondrial fragmentation and increased hypersensitivity to apoptosis.** (A) HeLa cells stably expressing Su9-DsRed were transfected with the indicated siRNA. Live images were obtained by fluorescence microscopy (a–e magnified images are shown as insets in b and e). EM of these manipulated cells are shown in f–j. (B) Onionlike mitochondrial inner membrane structures in *Opa1/Drp1* and *Opa1/Mff* double knockdown cells. (C) Percentages of cells with the indicated mitochondrial morphologies in various RNAi cells. Data were obtained from 100 cells in each of three independent experiments and represent mean ± SD. (D) HeLa cells were transfected with the indicated siRNA and then treated with actinomycin D in the presence of Z-VAD-FMK. Cells were fixed at the indicated time points, and cytochrome *c* release was detected by immunostaining. Data were obtained from 300 cells in each of three independent experiments and represent mean ± SD.

Mff RNAi cells, whereas *Opa1* RNAi cells had extensively fragmented mitochondria (Fig. 6, A and C; and Fig. S1 C), indicating that Mff limited *Opa1* RNAi–induced mitochondrial fission. Similar results were obtained for the simultaneous knockdown of *Drp1* and *Opa1*, suggesting that Mff and Drp1 mediated mitochondrial fission in a similar way. EM analysis revealed that both *Opa1/Drp1* and *Opa1/Mff* double RNAi cells had mitochondria with disrupted cristae structures (Fig. 6 A, h and i) or onionlike innermembrane structures (Fig. 6 B). In marked contrast, the *Opa1/hFis1* double RNAi cells displayed extensively fragmented mitochondria with disorganized cristae strongly resembling those in the *Opa1* RNAi cells (Fig. 6 A, j and g), confirming findings of a previous study on the *Opa1/hFis1* double RNAi cells (Lee et al., 2004) and indicating that hFis1 is not rate limiting in the Drp1- and Mff-dependent mitochondrial fission reaction. Together, these two independent assays strongly indicate that, whereas Mff is essential for Drp1-dependent mitochondrial fission, hFis1 seems to be dispensable for the reaction.

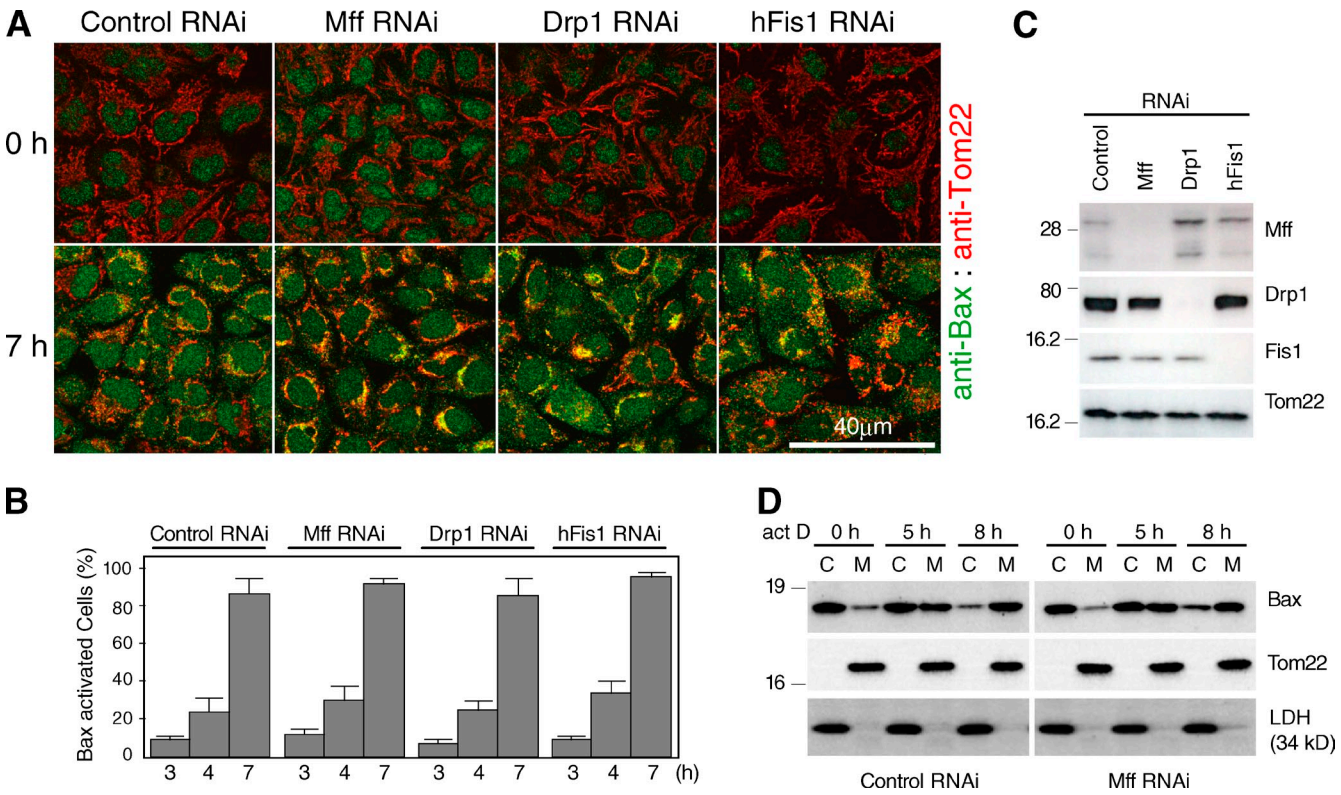

Figure 7. **Inhibition of Mff does not affect Bax activation during apoptosis.** (A) HeLa cells were transfected with the indicated siRNAs and then treated with actinomycin D (act D) in the presence of Z-VAD-FMK. The cells were immunostained with anti-Bax antibody (green) and anti-Tom22 antibody (red). (B) Time course of Bax activation. HeLa cells (n = 300) in A with mitochondria-targeted Bax were counted in three distinct fields, and data represent mean ± SD. (C) Cells in A were subjected to immunoblot analysis using the indicated antibodies. (D) *Mff* RNAi HeLa cells in A were fractionated to cytosol (C) and membrane (M) fractions, which were subjected to immunoblot analysis using the indicated antibodies. LDH, lactate dehydrogenase. Molecular mass is given in kilodaltons.

Cytochrome *c* release in *Opa1* RNAi cells is suppressed by knockdown of either *Drp1* or *Mff* but not *hFis1*

Because mitochondrial morphology is intertwined with apoptosis (Lee et al., 2004; Youle and Karbowski, 2005; Parone and Martinou, 2006; Arnoult 2007; Gandre-Babbe and van der Bliek, 2008; Suen et al., 2008; Wasilewski and Scorrano 2009), we assessed the contributions of Mff and hFis1 to actinomycin D–triggered cytochrome *c* release in the aforementioned cells. *Opa1* RNAi stimulated cytochrome *c* release, and additional knockdown of either *Drp1* or *Mff* strongly compromised the response to the same extent as in single *Drp1* or *Mff* RNAi cells (Fig. 6 D). In contrast, the response was not affected by *hFis1* RNAi or simultaneous RNAi of *Opa1* and *hFis1* (Fig. S3 C and Fig. 6 D), consistent with the aforementioned mitochondrial morphology response. As indicated in Fig. 6, both *Opa1* RNAi and *Opa1/hFis1* double RNAi cells had extensively fragmented mitochondria with disorganized cristae structure and released cytochrome *c*, whereas the cytochrome *c* release–incompetent *Opa1/Drp1* or *Opa1/Mff* double RNAi cells had enlarged mitochondria with disorganized cristae structures, suggesting that the fission step rather than cristae disorganization limits the release of cytochrome *c*. Of note, mitochondrial targeting of Bax and the release of Smac/DIABLO proceeded with the same kinetics as in the control cells irrespective of any of these manipulations (Fig. 7, A–D; unpublished data for Smac/DIABLO), confirming our previous observations (Ishihara et al., 2009). Together, these results suggest that mitochondrial fission reaction limits the cytochrome *c* release early during apoptosis. Consistent with this, overexpression of *Mff* induced extensive mitochondrial fragmentation concomitant with an increase in the cell sensitivity to apoptosis (unpublished data).

hFis1 is dispensable for fission in HCT116 cells

To investigate the role of hFis1 in mitochondrial fission explicitly, we conditionally knocked out *Fis1* in human HCT116 cells (see Materials and methods for detail; Fig. S4, A and B). As shown in Fig. 8 A, mitochondria exhibit normal morphology in *Fis1* CKO cells relative to the WT HCT116 cells. We also conducted FRAP analysis to quantitatively examine the mitochondrial connectivity in live cells. After photobleaching, the recovery rate of mito-YFP in *Fis1* CKO cells was indistinguishable from that in the WT cells (Fig. 8, B and C). Although we conducted our analysis as early as 3 d after Ad-Cre infection, there might still be a compensation effect by components of the mitochondrial fusion machinery to counter a reduced mitochondrial fission rate. To address this possibility, we performed mito-photoactivatable GFP analysis (Karbowski et al., 2006), and we found no significant difference in the mitochondrial fusion rate between *Fis1* CKO cells and the WT cells (Fig. 8 D), suggesting the absence of compensatory effects on mitochondrial fusion rate.

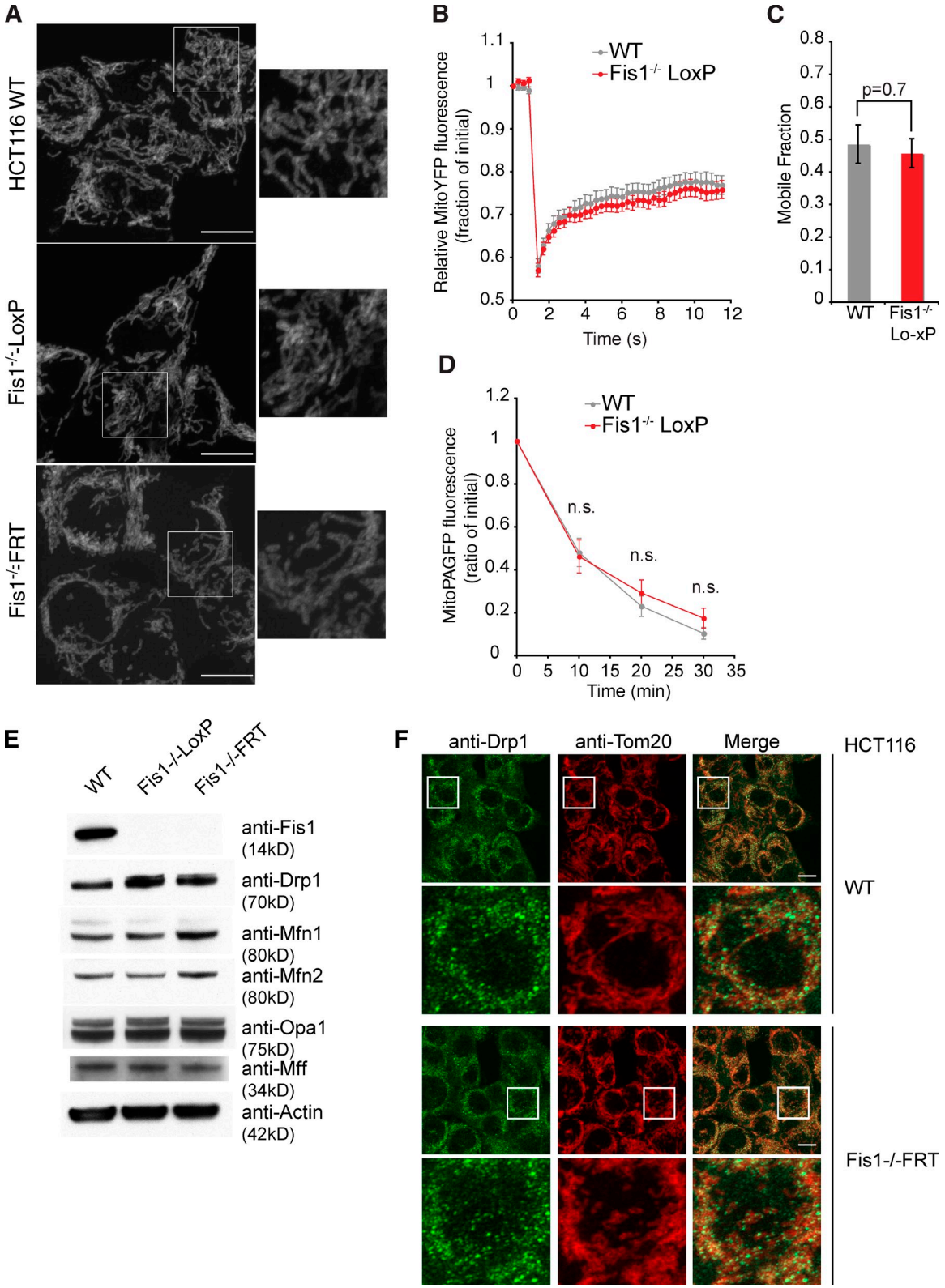

Figure 8. **Characterization of mitochondrial morphology in *Fis1* CKO cells.** (A) Comparison of mitochondrial morphology in WT and *Fis1* CKO cells immunostained with anti-Tom20 antibody. (B and C) The mitochondrial network connectivity assay showing FRAP curves (B) or mobile fractions (C) from either WT or *Fis1*$^{-/-}$-LoxP HCT116 cells was performed as in Fig. 1 (B and C). (D) Mitochondrial fusion rate in either WT or *Fis1*$^{-/-}$-LoxP HCT116 cells. A 1.88-µm circle containing multiple mitochondria was activated with a 413-nm laser, and images were acquired at 0, 10, 20, and 30 min after activation using the 488-nm laser. The fraction of remaining activated mitochondria was quantified using MetaMorph software (MDS Analytical Technologies). The mean ± SEM of 23 distinct photoactivated regions is plotted and is representative of three independent experiments. MitoPAGFP, mito-photoactivatable GFP. n.s., not significant. (E) Comparison of mitochondrial fission and fusion protein levels in WT and two sets of *Fis1* CKO cells. (F) Drp1 subcellular localization in *Fis1* CKO cells. In A and F, magnified images of the squared regions are shown. Bars, 10 µm.

Because the available anti-Fis1 antibody was generated from an N-terminal epitope, a potential truncated Fis1 protein could be produced and functional in our initial *Fis1* CKO cells given that the exon 2 was targeted. Therefore, we sought to make a second version of *Fis1* CKO in which no truncated Fis1 protein would be made (see Materials and methods for details; Fig. S4, C and D). To distinguish the two versions of *Fis1* CKO cells, we called the first version $Fis1^{-/-}$-LoxP and the second version $Fis1^{-/-}$–flippase recognition target (FRT). Nevertheless, mitochondrial morphology remained normal in this new version of *Fis1* CKO cells (Fig. 8 A).

Because many mammalian genes exhibit alternative splicing and certain aberrant splicing events have been reported to occur in KO cells but not in WT cells (Egger et al., 2006; Spada et al., 2007), we also investigated whether any functional *Fis1* transcripts were made in *Fis1* CKO cells, which might not be detectable by the antibody we used. There are nine alternative *hFis1* splicing variants all sharing exons 3–5 (although in different reading frames; Fig. S5 A). The *hFis1-001* transcript is the only one encoding a functional Fis1 protein. We performed 5′RACE using the GeneRacer kit to capture full-length 5′ ends of *hFis1* cDNAs in both the WT cells and $Fis1^{-/-}$-LoxP cells. The 5′RACE PCR products were cloned, and individual clones were sequenced. Among 20 clones obtained from the WT cells, nine contained the hFis1-001 transcript. In contrast, among 21 clones obtained from the $Fis1^{-/-}$-LoxP cells, no *hFis1-001* transcripts or *hFis1-001* transcripts containing the LoxP sequence (from the targeting allele) or other aberrant splicing variants were detected (Fig. S5 B), indicating that the *Fis1* CKO cells are truly null.

To see whether other mitochondrial fission and fusion protein levels were altered in the *Fis1* CKO cells owing to potential compensatory effects, we performed Western blotting to compare the expression levels of those proteins in the *Fis1* CKO cells and the WT HCT116 cells. Very similar expression levels of mitochondrial fusion proteins Mfn1, Mfn2, and Opa1 were detected in WT cells and the two versions of *Fis1* CKO cells (Fig. 8 E). Mitochondrial fission proteins Drp1 and Mff were not reduced in the *Fis1* CKO cells. In addition, immunofluorescence staining with anti-Drp1 antibody indicated that mitochondrial recruitment of Drp1 was not altered in *Fis1*-null cells (Fig. 8 F).

Fis1 RNAi in Fis1 CKO cells still causes mitochondria elongation

We also performed *Fis1* RNAi in HCT116 cells. Surprisingly, the same shRNA that was effective in HeLa cells (Lee et al., 2004) failed to knock down hFis1 levels in HCT116 cells (possibly because of sequence polymorphism between HeLa and HCT116 cells; Fig. 9 A, compare lane 1 with lane 6). However, this *Fis1* shRNA did induce the formation of elongated mitochondria to a similar extent to that seen in *Drp1* knockdown HCT116 cells (Fig. 9 B). Of note, such elongated mitochondria are likely caused by unusually enlarged cell size induced by this particular *hFis1* shRNA (Fig. 9 B). Unlike previous findings that *Fis1* RNAi also led to elongated peroxisomes in HeLa cells (Koch et al., 2005), such a phenotype was not observed in HCT116 cells using the same shRNA of Lee et al. (2004; unpublished data). To further rule out the possibility of the cell type–specific effect of *hFis1*, we tested four validated Fis1 shRNA from Sigma-Aldrich in both HeLa and HCT116 cells. These new sets of RNAi knocked down Fis1 protein level to >80%, but none of them affected mitochondrial morphology in either cell line (Fig. 9, C and D), consistent with our observations in *Fis1* KO cells and further indicating that hFis1 has no or a minor role in mitochondrial fission.

Mff RNAi, but not hFis1 RNAi and hFis1 CKO, stimulates peroxisomal tubular extension

Because mammalian peroxisomes and mitochondria have been shown to share components of the fission machinery, namely Drp1, hFis1, and Mff (Koch et al., 2005; Schrader, 2006; Waterham et al., 2007; Gandre-Babbe and van der Bliek, 2008), we reevaluated the effect of *hFis1* RNAi on peroxisomal morphology compared with that of *Mff* RNAi. *Mff* RNAi induced significant peroxisomal tubulation to a similar extent as *Drp1* RNAi, confirming a previous study of Gandre-Babbe and van der Bliek (2008; Fig. 10 A). However, no significant morphology changes were observed in *hFis1* RNAi cells. This was further corroborated by immunofluorescence microscopy of *hFis1* CKO human colon tumor cells (Fig. 10 B). Together, these results clearly indicate that Drp1 and Mff regulate peroxisomal fission, as is the case for mitochondrial fission. Contribution of Fis1 in Drp1-dependent peroxisomal fission seemed to be very low, if at all.

Discussion

Here, we demonstrate that Mff plays a key role in Drp1 recruitment. In yeast, mitochondrial fission is controlled by four genes: *Dnm1*, *Mdv1*, *Caf4*, and *Fis1*. Dnm1 is recruited to mitochondria by Fis1 via two adaptor proteins, Mdv1 and Caf4 (Tieu and Nunnari, 2000; Griffin et al., 2005; Zhang and Chan, 2007). Because both Dnm1 and Fis1 are homologues in mammals (Drp1 and Fis1 have been shown to mediate mitochondria fission as well), it is believed that the mechanism underlying mitochondria fission is conserved between yeast and mammals. However, there are some gaps that need to be filled. First, whereas Mdv1 and Caf4 have been shown to be essential for bridging the interaction between Dnm1 and yFis1, no homologues of these two adaptor proteins have been found in the mammalian genome. Second, although yFis1 is required for Dnm1 recruitment to mitochondria, knockdown of Fis1 in mammalian cells does not affect Drp1 recruitment to mitochondria. In this study, we present findings that help fill in the gaps: (a) hFis1 is dispensable for mitochondria and peroxisome fission in human cells; and (b) a novel mitochondria fission protein Mff is essential for Drp1 recruitment to mitochondria. Given that no Mff homologue exists in yeast (Gandre-Babbe and van der Bliek, 2008), our data suggest that new mechanisms or new components of mitochondrial fission machinery have evolved in mammals.

The role of Mff in Drp1-mediated mitochondrial fission is strongly supported by several lines of evidence. First, the ability of Mff to promote mitochondrial fission is strictly dependent on

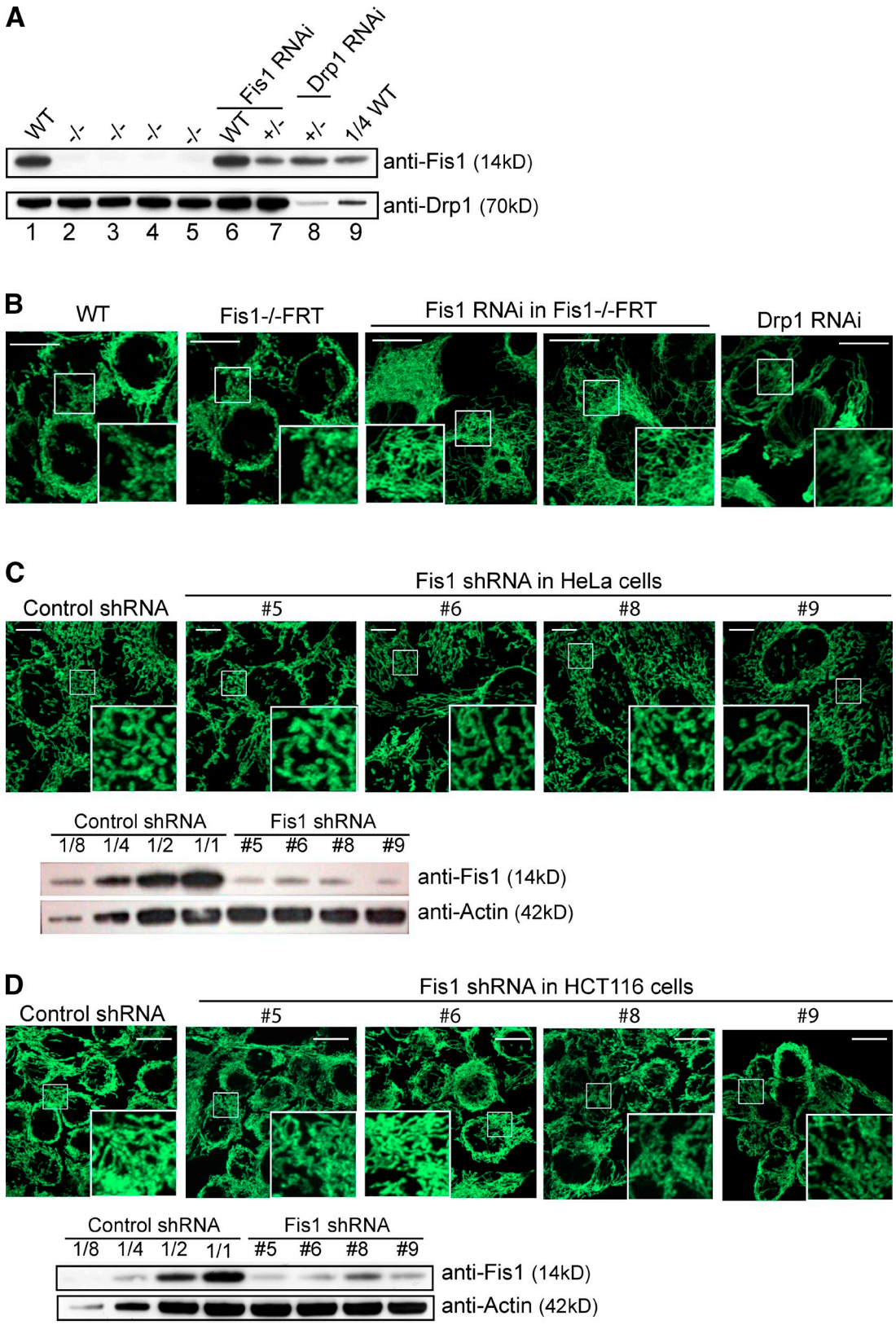

Figure 9. **Off-target effect of *Fis1* RNAi on mitochondrial morphology.** (A) Fis1 and Drp1 protein levels in the indicated RNAi cells. (B) Comparison of mitochondrial morphology in WT, *Fis1* CKO, and the indicated RNAi cells. Cells were immunostained with anti–cytochrome *c* antibody. (C and D) Comparison of mitochondrial morphology in lentivirus-infected control RNAi or *Fis1* RNAi HeLa (C) or HCT116 (D) cells immunostained with anti-Tom20 antibody. Knockdown level of each Fis1 shRNA was indicated by Western blotting. The insets show magnified images of the squared regions. Bars, 10 µm.

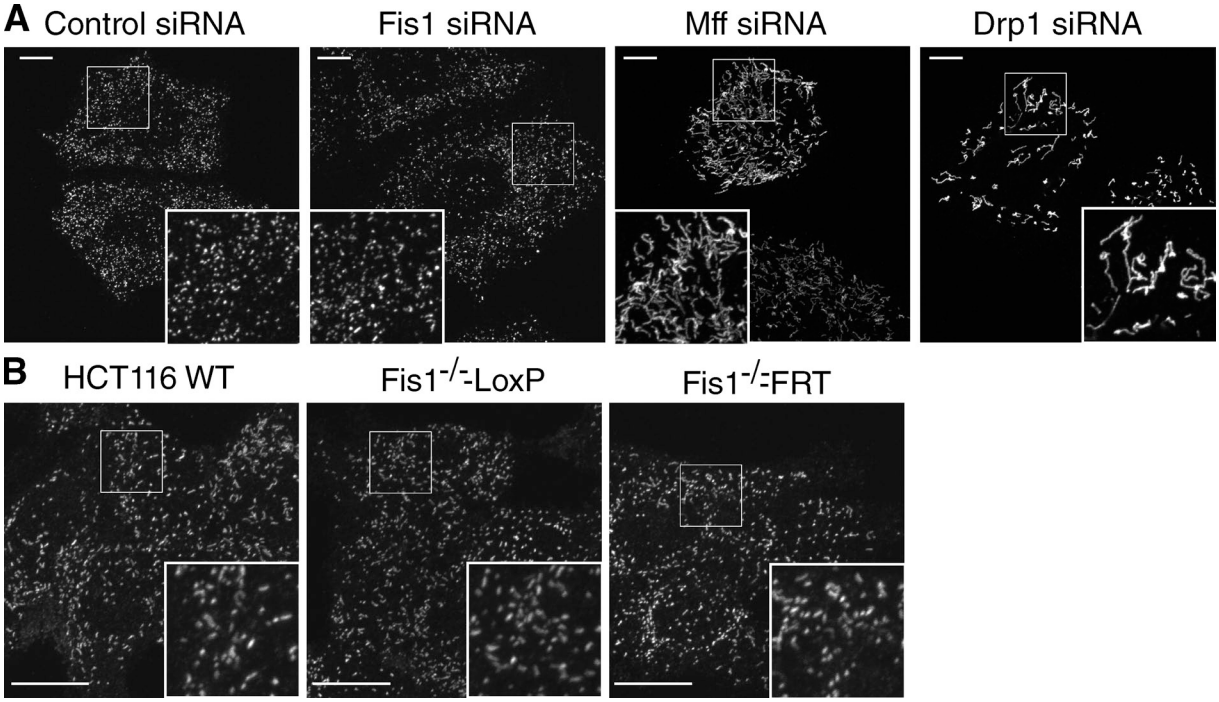

Figure 10. **Mff, but not hFis1, affects peroxisomal morphology.** (A) HeLa cells were transfected with the indicated siRNAs, and peroxisome morphology was revealed by immunostaining with anti-PMP70 antibody. (B) Peroxisome morphology in WT and *Fis1* CKO cells was detected as in A. The insets show magnified images of the squared regions. Bars, 10 µm.

Drp1 because overexpression of *Mff* fails to induce mitochondrial fission in *Drp1*$^{-/-}$ MEF cells, indicating that Mff acts through Drp1. Second, Drp1 remains in the cytosol and cannot be recruited to the mitochondria in Mff-depleted cells. Furthermore, direct interaction between Drp1 and Mff is detected both in vitro and in vivo. It was recently reported that the human patient Drp1 mutant A395D is defective in forming higher ordered assembly and mitochondrial recruitment (Chang et al., 2010). Corroborating the necessity of the Mff–Drp1 interaction, this mutant is also defective in binding to Mff. Based on this, it is worthy to test in the future whether Mff is responsible for Drp1 assembling into a higher order complex. Two other Drp1 mutants, G350D and G363D, exhibit similar defects as A395D (Chang et al., 2010), indicating that the middle domain of Drp1 might be mediating the interaction between Drp1 and Mff. Although the interaction is direct, it is likely transient and dynamic and possibly regulated by a GTP/GDP-bound form or other modifications of Drp1. If the interaction were stable, Drp1 should be constantly recruited to mitochondria by Mff. Consistent with a transient complex, the interaction between Drp1 and Mff cannot be detected without cross-linking both in vivo and in vitro. The transient nature of the Mff–Drp1 interaction likely explains the lack of a dominant-negative activity of the MffΔC mutant, which is strikingly similar to yeast Fis1ΔC, which does not exhibit a dominant-negative effect either (Mozdy et al., 2000). It is intriguing to speculate as to whether novel adaptor proteins have evolved to substitute for Mdv1/Caf4 in mammals or whether the adaptor proteins have been lost during evolution and Mff can fulfill all the functions of a receptor and an adaptor.

The normal mitochondrial morphology in the *Fis1* CKO HCT116 cells further indicates that hFis1 is either dispensable for mitochondria fission or there is an unknown redundant protein that can functionally substitute for hFis1. Mitochondrial fusion rates are indistinguishable between WT HCT116 cells and the *Fis1* CKO cells (Fig. 8 D), which is consistent with unaltered protein levels of the well-established mitochondrial fission and fusion proteins in the CKO cells (Fig. 8 E). All these data strongly indicated that the lack of mitochondrial morphological change in *Fis1* CKO cells was not caused by compensatory effects. It is noteworthy that all previous studies on the role of Fis1 in human mitochondrial and peroxisomal fission were shown with one single piece of RNAi (Yoon et al., 2003; Lee et al., 2004; Stojanovski et al., 2004; Koch et al., 2005). In contrast, we found that knockdown of *Fis1* by four new siRNAs and four new shRNAs (with a more effective knockdown level) fails to alter either mitochondrial or peroxisomal morphology. So, why is Fis1 not essential for mitochondrial fission in mammals? Although plant Fis1 orthologues have been shown to be required for mitochondrial fission (Zhang and Hu, 2008), deletion of *Fis1* and *Fis2* in *Caenorhabditis elegans* did not result in any detectable mitochondrial defects (Breckenridge et al., 2008). Moreover, hFis1 cannot rescue the phenotype of yeast *fis1Δ* cells (Stojanovski et al., 2004; Suzuki et al., 2005). Swapping the C-terminal domains between rat Fis1 and yeast Fis1p results in the loss of the ability to induce mitochondrial fission (Jofuku et al., 2005), indicating that either the two proteins are structurally divergent or act through different mechanisms.

What is the functional relation of Mff and hFis1? The most plausible possibility is that Mff functions as a Drp1 receptor and hFis1 functions downstream of Mff, where hFis1 modulates the assembly of fission foci containing Drp1, Mfn2, Bax, or Endophilin B1 and the subsequent severing process (Karbowski et al., 2004;

Lee et al., 2004; Suen et al., 2008; Benard and Karbowski, 2009). Another possibility might be that Mff and hFis1 are involved in distinct Drp1-dependent functions such as mitochondrial translocation. In mammalian cells, F-actin and the dynein/dynactin microtubule system function in Drp1 recruitment to the mitochondria (Varadi et al., 2004; DeVos et al., 2005). In yeast, Dnm1 often colocalizes with Num1 as punctate structures Fis1 independently and participates in the division and intracellular distribution of mitochondria (Cerveny et al., 2007a; Hammermeister et al., 2010). Finally, we cannot rule out the possibility that protein overexpression sometimes induces nonphysiological stress in the cells, which leads to changes in the mitochondrial morphology and localization, or apoptosis; i.e., overexpression of MOM proteins, including Tom20, induces perinuclear accumulation of fragmented mitochondria (Kanaji et al., 2000; Eura et al., 2003). Therefore, caution should be taken when interpreting data from overexpression studies.

In summary, our data solidify the differences observed in the mitochondrial fission process between yeast and metazoans so that new models might need to be conceptualized. Our data also emphasize the needs of identifying novel or missing factors involved in mammalian mitochondrial fission.

Materials and methods

Materials

Antibodies against Mff (Sigma-Aldrich; gift from A. van der Bliek, University of California, Los Angeles, CA; Gandre-Babbe and van der Bliek, 2008), Drp1, Opa1 (BD), Tom20 (Santa Cruz Biotechnology, Inc.), FLAG (M2; Sigma-Aldrich), lactate dehydrogenase, actin (Sigma-Aldrich), HA (Covance), cytochrome *c* (BD), and cleaved caspase-3 (Cell Signaling Technology) were purchased from the indicated vendors. Antibodies against Fis1 (Jofuku et al., 2005), Tom70 (Suzuki et al., 2002), and mitofilin (Eura et al., 2006) were described previously. Rabbit polyclonal antibodies against Mfn1 and Mfn2 were raised against recombinant truncated Mfn1 proteins (C terminal) and Mfn2 proteins (N terminal). March5 cDNA was a gift from S. Yanagi (Tokyo University of Pharmacology and Life Science, Tokyo, Japan). Actinomycin D (Sigma-Aldrich) was used at a final concentration of 10 µM. Z-VAD-FMK (Peptide Institute) was used at a final concentration of 100 µM. CCCP (Sigma-Aldrich) was used at a final concentration of 20 µM.

Cloning, RNAi, and mutagenesis

Mff cDNA was obtained with RT-PCR using total RNA isolated from MEF cells. The PCR product was cloned into the AflII and NotI sites of the pcDNA3.1 vector and sequenced to rule out mutations introduced by PCR. All truncation mutants of Mff were also cloned into AflII and NotI sites of the pcDNA3.1 vector using standard molecular biology techniques with PCR. A FLAG-tag sequence was inserted by PCR at the 5′ end of the sequence. To replace endogenous Mff with RNAi-resistant FLAG-Mff, the underlined nucleotides were changed to introduce a silent mutation in the Mff siRNA target sequence (Mff siRNA #2: 5′-AACGCTGACCTGGAACAAGGA-3′). *Mff* cDNA was also cloned into pNucScrIII, a vector containing humanized *Renilla reniformis* GFP (Agilent Technologies) with three tandem SV40 NLSs downstream of the IRES sequence to coexpress both humanized *Renilla* GFP and Mff. Fis1 and March5 constructs were also created by PCR using the appropriate cDNAs as templates and the appropriate combinations of forward and reverse oligonucleotide primers. All resulting PCR fragments were cloned into the appropriate restriction sites of the pNucScrIII vector (Oka et al., 2008). All constructs were confirmed by nucleotide sequencing and used for the assays.

Oligonucleotides for siRNA were made by QIAGEN. The three pairs of *Mff* siRNA oligonucleotides were based on the following sequences: 5′-ACCGATTTCTGCACCGGAGTA-3′ (*Mff* siRNA #1), 5′-AACGCTGACCTGGAACAAGGA-3′ (*Mff* siRNA #2), and 5′-CTGAGCAGTTCTGCAGTAACA-3′ (*Mff* siRNA #3). The results shown in the figures were obtained with the second pair, but the third pair was equally effective (Fig. S1 A). The four pairs of *hFis1* siRNA oligonucleotides were based on the following sequences: 5′-AACGAGCTGGTGTCTGTGGAG-3′ (*hFis1* siRNA #1), 5′-AAAGGCCATGAAGAAAGATGG-3′ (*hFis1* siRNA #2), 5′-CCGGCTCAAGGAATACGAGAA-3′ (*hFis1* siRNA #3), and 5′-AAGGCCATGAAGAAAGATGGA-3′ (*hFis1* siRNA #4). The results shown were obtained with the first pair, but the other pairs were equally effective (Fig. S3, A–C). Pairs of *Drp1*, *March5*, and *Opa1* siRNAs were based on the sequences 5′-AAGCAGAAGAATGGGGTAAAT-3′, 5′-AATCTTGGGTGGAATTGCGTT-3′, and 5′-AACACGTTTTAACCTTGAAAC-3′, respectively.

For RNAi work in HCT116 cells, scrambled, *Fis1*, and *Drp1* shRNA were constructed as previously described (Lee et al., 2004) and recloned into the pREP4-puro vector (obtained from F. Bunz, Johns Hopkins University, Baltimore, MD; Liu et al., 2001) because HCT116 cells are resistant to hygromycin selection. The shRNA plasmids were transfected into HCT116 or *Fis1* CKO cells. After 36 h, cells were selected with 0.5 µg/ml puromycin for 3 d (when 100% of nontransfected control cells were killed) and then maintained in 0.3 µg/ml puromycin. Four validated Fis1 shRNAs were purchased from Sigma-Aldrich in lentiviral particles (titer between ∼2.7 and 3.4 × 10^7 TU/ml). The target sequences for each *Fis1* shRNA are 5′-CAAGAGCACGCAGTTTGAGT-3′ (#5, clone TRCN0000155375), 5′-GCTCATTGACAAGGCCATGA-3′ (#6, clone TRCN0000155276), 5′-GTACAATGATGACATCCGTA-3′ (#8, clone TRCN0000151188), and 5′-GAACTACCGGCTCAAGGAAT-3′ (#9, clone TRCN0000154799). HeLa and HCT16 cells were infected with 30 µl of lentiviral particles in the presence of 4 µg/ml polybrene (Sigma-Aldrich) for 2 d and selected with puromycin for 3 d before immunofluorescence staining analysis.

Cell culture and transfection

HeLa cells, a Su9-DsRed–expressing cell line, a FLAG-Drp1– or HA-Drp1–expressing cell line, and MEF cells were maintained at 37°C in DME supplemented with 10% FBS. HCT116 cells were purchased from American Type Culture Collection and cultured in McCoy's 5A medium supplemented with 10% FBS, 1 mM glutamine, and nonessential amino acids. AAV-293 cells (Agilent Technologies) were cultured in DME medium supplemented with 10% FBS, 1 mM glutamine, nonessential amino acids, 1 mM sodium pyruvate, and 10 mM Hepes buffer solution. DNA transfection was performed using FuGENE HD (Roche) according to the manufacturer's instructions for HeLa cells and Lipofectamine LTX (Invitrogen) for HCT116 cells. Cells were transfected with siRNA duplexes at a concentration of 75 pM by Lipofectamine 2000 (Invitrogen). At 24 h after the initial treatment, the second siRNA transfection was performed, and cells were grown for 48 h. At 72 h after initial treatment, cells were fixed with 4% PFA for indirect immunofluorescence study or lysed with SDS-loading buffer for immunoblotting. For cotransfections with overexpression constructs, the siRNA-transfected cells were split after 72 h and retransfected with 75 pM siRNA oligonucleotides and the expression plasmids. After 24 h, these cells were used for the assays.

Gene targeting

To make the conditional gene-targeting construct (CKO), two 1-kb sequences flanking exon 2 of the human Fis1 gene were PCR amplified from HCT116 genomic DNA with DNA polymerase (Phusion; New England Biolabs, Inc.). The 5′ homologue arm (HA) was ligated with Neomycin (Neo) cassette cut out from pSEPT (obtained from K. Zhao, National Heart, Lung, and Blood Institute, National Institutes of Health, Bethesda, MD; Topaloglu et al., 2005) and cloned into pBluescript SK II. The exon 2 was PCR amplified with two LoxP sites introduced in the two PCR primers, resulting in exon 2 flanked with LoxP sites. This PCR fragment was ligated with the 3′ homologue arm and cloned into pBluescript SK II. The inserts containing the 5′ arm and Neo cassette and the floxed exon 2 and 3′ arm were cut out, respectively, and ligated together with the pAAV-MCS vector (Agilent Technologies) to make the final CKO construct pAAV-Fis1 CKO. To make the constitutive gene-targeting construct, the 5′ arm and 3′ arm were PCR amplified and ligated together with pAAV-MCS, and the Neo cassette was cut out from the pSEPT vector to make the pAAV-Fis1 KO construct.

The pAAV-Fis1 CKO and pAAV-Fis1 KO plasmid were cotransfected with pAAV-RC and pHelper into AAV-293 cells for virus packaging according to the manufacturer's instruction (Agilent Technologies). 3 × 10^6 HCT116 cells were infected with the aforementioned virus. After 24 h, the cells were harvested and plated into four 96-well plates containing 0.5 mg/ml G418 for selection. After 7–10 d, the single colonies were transferred to 24-well plates, and genomic DNA was isolated from each clone for PCR screening. Positive clones were expanded and frozen. To remove the Neo cassette, targeted clones were either infected with adenovirus Ad-Cre–GFP (Vector Laboratories) or transiently transfected with pPGKFLPobpA (plasmid 13793; Addgene). Cells were then serial diluted

to obtain single colonies. Single colonies were subsequently duplicated, tested for G418 sensitivity, and expanded.

The first allele contains two FRT sites flanking the Neo cassette and two LoxP sites flanking exon 2 of Fis1. The Neo cassette harbors a synthetic intron and a synthetic splicing acceptor followed by an IRES, Neo ORF, and a polyadenylation signal sequence (Topaloglu et al., 2005). After integrating into the chromosomal locus of Fis1 by homologous recombination, the exogenously introduced Neo ORF was spliced into the transcript of the Fis1 gene. This transcript terminated at the poly(A) site after Neo ORF, resulting in inactivation of the Fis1 gene. However, after removal of the Neo cassette by Flpo recombinase (Raymond and Soriano, 2007), the flox allele became active because the LoxP-flanked exon 2 could be correctly spliced into the Fis1 gene. The second allele was targeted with a constitutive targeting vector, which introduced several base deletions and stop codons. The *Fis1*$^{flox/-}$ cells behaved like heterozygotes and were indistinguishable from WT cells. After Ad-Cre–GFP infection, the exon 2 in the flox allele was excised and resulted in homozygosity (Fig. S4 A). We harvested cells 3–5 d after Ad-Cre infection to ensure complete turnover of the endogenous Fis1 protein.

To make the second version of *Fis1* CKO, the second allele was again targeted with the constitutive targeting vector, but the IRES–Neo cassette was flanked by two FRT sites instead of LoxP sites (Fig. S3 C). If the *Fis1*$^{flox/-}$ cells were infected with Ad-Cre, the flox allele would become a null allele because of the excision of the exon 2. The constitutively targeted allele would remain gene trapped (as the IRES–Neo cassette could not be excised), and no truncated Fis1 protein would be produced.

Immunoblotting and immunofluorescence microscopy

Immunoblotting was performed as described previously (Setoguchi et al., 2006). For immunofluorescence microscopy, cells were grown on glass coverslips and then fixed for 15 min at room temperature with prewarmed 4% PFA. Cells were permeabilized for 5 min with 1% Triton X-100 in PBS and incubated with primary antibodies. After incubation with Alexa Fluor–conjugated secondary antibodies (Invitrogen), images were acquired with a 63× oil immersion objective on an Axiovert 200M microscope (Carl Zeiss, Inc.; Fig. 1, A and C; Fig. 2, D and E; Fig. 3 A; Fig. 4 B; Fig. 5, A, E, and F; and Fig. S1, B and D) or on a confocal microscope (Radiance 2000; Bio-Rad Laboratories; Fig. 1 F; Fig. 2, A and C; Fig. 3, B, C, F, and H; Fig. 5 B; Fig. 6 A; Fig. 7 A; Fig. 8 A; Fig. S2 B; and Fig. S3).

Expression and purification of recombinant Drp1 and Mff

PCR products for full-length Drp1 and Mff lacking a C-terminal TMD (MffΔC) were cloned into the EcoR1–Not1 site of pGEX6P-1 (GE Healthcare). Drp1-A395D mutant was constructed in pGEX6P-1/Drp1 using PCR with primers encoding point mutations. Drp1, Drp1-A395D, and MffΔC were expressed as GST fusion proteins in *Escherichia coli* and were purified with glutathione–Sepharose beads (GE Healthcare) as previously described (Otera et al., 2002). Drp1, Drp1-A395D, and MffΔC were isolated from thus purified GST fusion proteins by cleaving with protease (PreScission; GE Healthcare) according to the manufacturer's protocol.

Chemical cross-linking and immunoprecipitation

10^6 HeLa cells were transfected with HA-Drp1, FLAG-Mff, and FLAG-hFis1 in various combinations. After 24 h, the cells were treated with a cross-linker, 0.75 mM DSP, for 30 min. The cells were lysed either in 1 ml of solubilization buffer (50 mM Tris-HCl, pH 7.5, containing 1% digitonin; mild condition) or 200 µl of solubilization buffer (50 mM Tris-HCl, pH 7.5, containing 1% SDS; stringent condition). The latter extract was incubated at 95°C for 5 min and then diluted 10-fold with immunoprecipitation buffer (50 mM Tris-HCl, pH 7.5, containing 150 mM NaCl, 1% Triton X-100, and protease inhibitor). Both lysates were clarified by centrifugation, and the supernatants were subjected to immunoprecipitation with anti-FLAG antibody. Immunoprecipitates were analyzed by SDS-PAGE and immunoblotting with antibodies to HA and FLAG. For direct binding between Drp1 and MffΔC, purified Drp1 and MffΔC were incubated in PBS containing 1 mM DSP at 30°C for 30 min. After termination of the reaction by 50 mM Tris-HCl, pH 7.5, reaction mixtures were subjected to immunoprecipitation with anti-Drp1 antibody in the presence of 1% Triton X-100. Immunoprecipitates were washed with PBS containing 1% Triton X-100 and analyzed by SDS-PAGE and subsequent immunoblotting with antibodies to Drp1 and Mff.

Cell fractionation

Cells transfected with siRNAs for control, Mff, or hFis1 were washed with PBS and collected by centrifugation at 800 *g* for 5 min. The cells were washed once with homogenization buffer (10 mM Hepes-KOH, pH 7.5, containing 0.25 M sucrose), homogenized in 1 ml of homogenization buffer by passing through a 27-gauge needle 10 times, and then centrifuged at 1,000 *g* for 10 min to obtain a postnuclear supernatant. The postnuclear supernatant was centrifuged at 8,000 *g* for 10 min to obtain a mitochondria-rich heavy membrane fraction. The resultant supernatant was further centrifuged at 100,000 *g* for 15 min to obtain the cytosol fraction.

EM

For EM, cells were fixed in 4% PFA and 1% glutaraldehyde at 25°C for 30 min and analyzed as described previously (Eura et al., 2003).

5′RACE

Total RNA was isolated with the RNeasy Mini kit (QIAGEN). 5′RACE was performed with a GeneRacer kit (Invitrogen) according to the manufacturer's instruction with a gene-specific primer, hFis1-GSP1 (5′-TCCGATGAGTCCGGCCAGTCC-3′). Nested PCR was performed with another gene-specific primer, hFis1-GSP2 (5′-CCCACGAGTCCATCTTTCTT-3′). The PCR products were cloned into the zero-blunt TOPO vector (Invitrogen), and positive clones were sequenced to confirm the nature of different splicing variants.

Mitochondrial photoactivation fusion assay

After cells were transfected using Lipofectamine LTX (HCT116) or Fugene 6 (HeLa) with mito-photoactivatable GFP (Karbowski et al., 2006), a small circular region of interest (ROI; 1.88 µm) containing multiple mitochondria was activated using a 413-nm laser, and the remaining portion of the experiment was performed as previously described (Cleland et al., 2010).

Mitochondrial connectivity FRAP assay

After cells were transfected with mito-YFP, a 36-µm by 18-µm rectangle was imaged with the 100× objective (zoom 2.5) before and after a six-iteration photobleach of a 2.1-µm circle placed over multiple mitochondria, and the remaining portion of the experiment was performed as previously described (Cleland et al., 2010).

Online supplemental material

Fig. S1 shows the characterization of Mff siRNA. Fig. S2 shows raw data and the circular ROI on mitochondria for bleaching. Fig. S3 shows the characterization of hFis1 siRNA. Fig. S4 depicts the generation of two different versions of conditional Fis1 KO cells. Fig. S5 demonstrates that no functional hFis1 transcripts exist in Fis1 CKO cells. Online supplemental material is available at http://www.jcb.org/cgi/content/full/jcb.201007152/DC1.

We thank Toshihiko Oka and Naotada Ishihara for their comments and discussion of this manuscript. We are grateful to Fred Bunz for technical assistance.

This work was supported by grants from the Ministry of Education, Science, and Culture of Japan and in part by the Intramural Research Program of the National Institute of Neurological Disorders and Stroke, National Institutes of Health.

Submitted: 27 July 2010
Accepted: 12 November 2010

References

Alexander, C., M. Votruba, U.E. Pesch, D.L. Thiselton, S. Mayer, A. Moore, M. Rodriguez, U. Kellner, B. Leo-Kottler, G. Auburger, et al. 2000. OPA1, encoding a dynamin-related GTPase, is mutated in autosomal dominant optic atrophy linked to chromosome 3q28. *Nat. Genet.* 26:211–215. doi:10.1038/79944

Arnoult, D. 2007. Mitochondrial fragmentation in apoptosis. *Trends Cell Biol.* 17:6–12. doi:10.1016/j.tcb.2006.11.001

Benard, G., and M. Karbowski. 2009. Mitochondrial fusion and division: regulation and role in cell viability. *Semin. Cell Dev. Biol.* 20:365–374. doi:10.1016/j.semcdb.2008.12.012

Breckenridge, D.G., B.H. Kang, D. Kokel, S. Mitani, L.A. Staehelin, and D. Xue. 2008. *Caenorhabditis elegans* drp-1 and fis-2 regulate distinct cell-death execution pathways downstream of ced-3 and independent of ced-9. *Mol. Cell.* 31:586–597. doi:10.1016/j.molcel.2008.07.015

Cerveny, K.L., S.L. Studer, R.E. Jensen, and H. Sesaki. 2007a. Yeast mitochondrial division and distribution require the cortical num1 protein. *Dev. Cell.* 12:363–375. doi:10.1016/j.devcel.2007.01.017

Cerveny, K.L., Y. Tamura, Z. Zhang, R.E. Jensen, and H. Sesaki. 2007b. Regulation of mitochondrial fusion and division. *Trends Cell Biol.* 17:563–569. doi:10.1016/j.tcb.2007.08.006

Chan, D.C. 2006. Mitochondrial fusion and fission in mammals. *Annu. Rev. Cell Dev. Biol.* 22:79–99. doi:10.1146/annurev.cellbio.22.010305.104638

Chang, C.-R., C.M. Manlandro, D. Arnoult, J. Stadler, A.E. Posey, R.B. Hill, and C. Blackstone. 2010. A lethal *de novo* mutation in the middle domain of the dynamin-related GTPase Drp1 impairs higher order assembly and mitochondrial division. *J. Biol. Chem.* 285:32494–32503. doi:10.1074/jbc.M110.142430

Cleland, M.M., K.L. Norris, M. Karbowski, C. Wang, D.F. Suen, S. Jiao, N.M. George, X. Luo, Z. Li, and R.J. Youle. 2010. Bcl-2 family interaction with the mitochondrial morphogenesis machinery. *Cell Death Differ.* doi:10.1038/cdd.2010.89

Delettre, C., G. Lenaers, J.M. Griffoin, N. Gigarel, C. Lorenzo, P. Belenguer, L. Pelloquin, J. Grosgeorge, C. Turc-Carel, E. Perret, et al. 2000. Nuclear gene OPA1, encoding a mitochondrial dynamin-related protein, is mutated in dominant optic atrophy. *Nat. Genet.* 26:207–210. doi:10.1038/79936

De Vos, K.J., V.J. Allan, A.J. Grierson, and M.P. Sheetz. 2005. Mitochondrial function and actin regulate dynamin-related protein 1-dependent mitochondrial fission. *Curr. Biol.* 15:678–683. doi:10.1016/j.cub.2005.02.064

Egger, G., S. Jeong, S.G. Escobar, C.C. Cortez, T.W. Li, Y. Saito, C.B. Yoo, P.A. Jones, and G. Liang. 2006. Identification of DNMT1 (DNA methyltransferase 1) hypomorphs in somatic knockouts suggests an essential role for DNMT1 in cell survival. *Proc. Natl. Acad. Sci. USA.* 103:14080–14085. doi:10.1073/pnas.0604602103

Eura, Y., N. Ishihara, S. Yokota, and K. Mihara. 2003. Two mitofusin proteins, mammalian homologues of FZO, with distinct functions are both required for mitochondrial fusion. *J. Biochem.* 134:333–344. doi:10.1093/jb/mvg150

Eura, Y., N. Ishihara, T. Oka, and K. Mihara. 2006. Identification of a novel protein that regulates mitochondrial fusion by modulating mitofusin (Mfn) protein function. *J. Cell Sci.* 119:4913–4925. doi:10.1242/jcs.03253

Frezza, C., S. Cipolat, O. Martins de Brito, M. Micaroni, G.V. Beznoussenko, T. Rudka, D. Bartoli, R.S. Polishuck, N.N. Danial, B. De Strooper, and L. Scorrano. 2006. OPA1 controls apoptotic cristae remodeling independently from mitochondrial fusion. *Cell.* 126:177–189. doi:10.1016/j.cell.2006.06.025

Gandre-Babbe, S., and A.M. van der Bliek. 2008. The novel tail-anchored membrane protein Mff controls mitochondrial and peroxisomal fission in mammalian cells. *Mol. Biol. Cell.* 19:2402–2412. doi:10.1091/mbc.E07-12-1287

Griffin, E.E., J. Graumann, and D.C. Chan. 2005. The WD40 protein Caf4p is a component of the mitochondrial fission machinery and recruits Dnm1p to mitochondria. *J. Cell Biol.* 170:237–248. doi:10.1083/jcb.200503148

Hammermeister, M., K. Schödel, and B. Westermann. 2010. Mdm36 is a mitochondrial fission-promoting protein in *Saccharomyces cerevisiae*. *Mol. Biol. Cell.* 21:2443–2452. doi:10.1091/mbc.E10-02-0096

Hoppins, S., L. Lackner, and J. Nunnari. 2007. The machines that divide and fuse mitochondria. *Annu. Rev. Biochem.* 76:751–780. doi:10.1146/annurev.biochem.76.071905.090048

Ishihara, N., Y. Fujita, T. Oka, and K. Mihara. 2006. Regulation of mitochondrial morphology through proteolytic cleavage of OPA1. *EMBO J.* 25:2966–2977. doi:10.1038/sj.emboj.7601184

Ishihara, N., M. Nomura, A. Jofuku, H. Kato, S.O. Suzuki, K. Masuda, H. Otera, Y. Nakanishi, I. Nonaka, Y. Goto, et al. 2009. Mitochondrial fission factor Drp1 is essential for embryonic development and synapse formation in mice. *Nat. Cell Biol.* 11:958–966. doi:10.1038/ncb1907

James, D.I., P.A. Parone, Y. Mattenberger, and J.-C. Martinou. 2003. hFis1, a novel component of the mammalian mitochondrial fission machinery. *J. Biol. Chem.* 278:36373–36379. doi:10.1074/jbc.M303758200

Jofuku, A., N. Ishihara, and K. Mihara. 2005. Analysis of functional domains of rat mitochondrial Fis1, the mitochondrial fission-stimulating protein. *Biochem. Biophys. Res. Commun.* 333:650–659. doi:10.1016/j.bbrc.2005.05.154

Kanaji, S., J. Iwahashi, Y. Kida, M. Sakaguchi, and K. Mihara. 2000. Characterization of the signal that directs Tom20 to the mitochondrial outer membrane. *J. Cell Biol.* 151:277–288. doi:10.1083/jcb.151.2.277

Karbowski, M., and R.J. Youle. 2003. Dynamics of mitochondrial morphology in healthy cells and during apoptosis. *Cell Death Differ.* 10:870–880. doi:10.1038/sj.cdd.4401260

Karbowski, M., S.-Y. Jeong, and R.J. Youle. 2004. Endophilin B1 is required for the maintenance of mitochondrial morphology. *J. Cell Biol.* 166:1027–1039. doi:10.1083/jcb.200407046

Karbowski, M., K.L. Norris, M.M. Cleland, S.Y. Jeong, and R.J. Youle. 2006. Role of Bax and Bak in mitochondrial morphogenesis. *Nature.* 443:658–662. doi:10.1038/nature05111

Karbowski, M., A. Neutzner, and R.J. Youle. 2007. The mitochondrial E3 ubiquitin ligase MARCH5 is required for Drp1 dependent mitochondrial division. *J. Cell Biol.* 178:71–84. doi:10.1083/jcb.200611064

Koch, A., Y. Yoon, N.A. Bonekamp, M.A. McNiven, and M. Schrader. 2005. A role for Fis1 in both mitochondrial and peroxisomal fission in mammalian cells. *Mol. Biol. Cell.* 16:5077–5086. doi:10.1091/mbc.E05-02-0159

Lee, Y.-J., S.-Y. Jeong, M. Karbowski, C.L. Smith, and R.J. Youle. 2004. Roles of the mammalian mitochondrial fission and fusion mediators Fis1, Drp1, and Opa1 in apoptosis. *Mol. Biol. Cell.* 15:5001–5011. doi:10.1091/mbc.E04-04-0294

Liu, R., H. Liu, X. Chen, M. Kirby, P.O. Brown, and K. Zhao. 2001. Regulation of CSF1 promoter by the SWI/SNF-like BAF complex. *Cell.* 106:309–318. doi:10.1016/S0092-8674(01)00446-9

McBride, H.M., M. Neuspiel, and S. Wasiak. 2006. Mitochondria: more than just a powerhouse. *Curr. Biol.* 16:R551–R560. doi:10.1016/j.cub.2006.06.054

Mozdy, A.D., J.M. McCaffery, and J.M. Shaw. 2000. Dnm1p GTPase-mediated mitochondrial fission is a multi-step process requiring the novel integral membrane component Fis1p. *J. Cell Biol.* 151:367–380. doi:10.1083/jcb.151.2.367

Niemann, A., M. Ruegg, V. La Padula, A. Schenone, and U. Suter. 2005. Ganglioside-induced differentiation associated protein 1 is a regulator of the mitochondrial network: new implications for Charcot-Marie-Tooth disease. *J. Cell Biol.* 170:1067–1078. doi:10.1083/jcb.200507087

Oka, T., T. Sayano, S. Tamai, S. Yokota, H. Kato, G. Fujii, and K. Mihara. 2008. Identification of a novel protein MICS1 that is involved in maintenance of mitochondrial morphology and apoptotic release of cytochrome c. *Mol. Biol. Cell.* 19:2597–2608. doi:10.1091/mbc.E07-12-1205

Okamoto, K., and J.M. Shaw. 2005. Mitochondrial morphology and dynamics in yeast and multicellular eukaryotes. *Annu. Rev. Genet.* 39:503–536. doi:10.1146/annurev.genet.38.072902.093019

Olichon, A., L. Baricault, N. Gas, E. Guillou, A. Valette, P. Belenguer, and G. Lenaers. 2003. Loss of OPA1 perturbates the mitochondrial inner membrane structure and integrity, leading to cytochrome c release and apoptosis. *J. Biol. Chem.* 278:7743–7746. doi:10.1074/jbc.C200677200

Otera, H., K. Setoguchi, M. Hamasaki, T. Kumashiro, N. Shimizu, and Y. Fujiki. 2002. Peroxisomal targeting signal receptor Pex5p interacts with cargoes and import machinery components in a spatiotemporally differentiated manner: conserved Pex5p WXXXF/Y motifs are critical for matrix protein import. *Mol. Cell. Biol.* 22:1639–1655. doi:10.1128/MCB.22.6.1639-1655.2002

Parone, P.A., and J.-C. Martinou. 2006. Mitochondrial fission and apoptosis: an ongoing trial. *Biochim. Biophys. Acta.* 1763:522–530. doi:10.1016/j.bbamcr.2006.04.005

Raymond, C.S., and P. Soriano. 2007. High-efficiency FLP and PhiC31 site-specific recombination in mammalian cells. *PLoS One.* 2:e162. doi:10.1371/journal.pone.0000162

Robert, A., M.-J. Miron, C. Champagne, M.-C. Gingras, P.E. Branton, and J.N. Lavoie. 2002. Distinct cell death pathways triggered by the adenovirus early region 4 ORF 4 protein. *J. Cell Biol.* 158:519–528. doi:10.1083/jcb.200201106

Santel, A., and M.T. Fuller. 2001. Control of mitochondrial morphology by a human mitofusin. *J. Cell Sci.* 114:867–874.

Schrader, M. 2006. Shared components of mitochondrial and peroxisomal division. *Biochim. Biophys. Acta.* 1763:531–541. doi:10.1016/j.bbamcr.2006.01.004

Scorrano, L., M. Ashiya, K. Buttle, S. Weiler, S.A. Oakes, C.A. Mannella, and S.J. Korsmeyer. 2002. A distinct pathway remodels mitochondrial cristae and mobilizes cytochrome c during apoptosis. *Dev. Cell.* 2:55–67. doi:10.1016/S1534-5807(01)00116-2

Setoguchi, K., H. Otera, and K. Mihara. 2006. Cytosolic factor- and TOM-independent import of C-tail-anchored mitochondrial outer membrane proteins. *EMBO J.* 25:5635–5647. doi:10.1038/sj.emboj.7601438

Smirnova, E., L. Griparic, D.L. Shurland, and A.M. van der Bliek. 2001. Dynamin-related protein Drp1 is required for mitochondrial division in mammalian cells. *Mol. Biol. Cell.* 12:2245–2256.

Spada, F., A. Haemmer, D. Kuch, U. Rothbauer, L. Schermelleh, E. Kremmer, T. Carell, G. Längst, and H. Leonhardt. 2007. DNMT1 but not its interaction with the replication machinery is required for maintenance of DNA methylation in human cells. *J. Cell Biol.* 176:565–571. doi:10.1083/jcb.200610062

Stojanovski, D., O.S. Koutsopoulos, K. Okamoto, and M.T. Ryan. 2004. Levels of human Fis1 at the mitochondrial outer membrane regulate mitochondrial morphology. *J. Cell Sci.* 117:1201–1210. doi:10.1242/jcs.01058

Suen, D.-F., K.L. Norris, and R.J. Youle. 2008. Mitochondrial dynamics and apoptosis. *Genes Dev.* 22:1577–1590. doi:10.1101/gad.1658508

Suzuki, H., M. Maeda, and K. Mihara. 2002. Characterization of rat TOM70 as a receptor of the preprotein translocase of the mitochondrial outer membrane. *J. Cell Sci.* 115:1895–1905.

Suzuki, M., S.Y. Jeong, M. Karbowski, R.J. Youle, and N. Tjandra. 2003. The solution structure of human mitochondria fission protein Fis1

reveals a novel TPR-like helix bundle. *J. Mol. Biol.* 334:445–458. doi:10.1016/j.jmb.2003.09.064

Suzuki, M., A. Neutzner, N. Tjandra, and R.J. Youle. 2005. Novel structure of the N terminus in yeast Fis1 correlates with a specialized function in mitochondrial fission. *J. Biol. Chem.* 280:21444–21452. doi:10.1074/jbc.M414092200

Tieu, Q., and J. Nunnari. 2000. Mdv1p is a WD repeat protein that interacts with the dynamin-related GTPase, Dnm1p, to trigger mitochondrial division. *J. Cell Biol.* 151:353–366. doi:10.1083/jcb.151.2.353

Topaloglu, O., P.J. Hurley, O. Yildirim, C.I. Civin, and F. Bunz. 2005. Improved methods for the generation of human gene knockout and knockin cell lines. *Nucleic Acids Res.* 33:e158. doi:10.1093/nar/gni160

Varadi, A., L.I. Johnson-Cadwell, V. Cirulli, Y. Yoon, V.J. Allan, and G.A. Rutter. 2004. Cytoplasmic dynein regulates the subcellular distribution of mitochondria by controlling the recruitment of the fission factor dynamin-related protein-1. *J. Cell Sci.* 117:4389–4400. doi:10.1242/jcs.01299

Wasiak, S., R. Zunino, and H.M. McBride. 2007. Bax/Bak promote sumoylation of DRP1 and its stable association with mitochondria during apoptotic cell death. *J. Cell Biol.* 177:439–450. doi:10.1083/jcb.200610042

Wasilewski, M., and L. Scorrano. 2009. The changing shape of mitochondrial apoptosis. *Trends Endocrinol. Metab.* 20:287–294. doi:10.1016/j.tem.2009.03.007

Waterham, H.R., J. Koster, C.W.T. van Roermund, P.A.W. Mooyer, R.J.A. Wanders, and J.V. Leonard. 2007. A lethal defect of mitochondrial and peroxisomal fission. *N. Engl. J. Med.* 356:1736–1741. doi:10.1056/NEJMoa064436

Yoon, Y., E.W. Krueger, B.J. Oswald, and M.A. McNiven. 2003. The mitochondrial protein hFis1 regulates mitochondrial fission in mammalian cells through an interaction with the dynamin-like protein DLP1. *Mol. Cell. Biol.* 23:5409–5420. doi:10.1128/MCB.23.15.5409-5420.2003

Youle, R.J., and M. Karbowski. 2005. Mitochondrial fission in apoptosis. *Nat. Rev. Mol. Cell Biol.* 6:657–663. doi:10.1038/nrm1697

Zhang, X.C., and J.P. Hu. 2008. FISSION1A and FISSION1B proteins mediate the fission of peroxisomes and mitochondria in *Arabidopsis*. *Mol Plant.* 1:1036–1047. doi:10.1093/mp/ssn056

Zhang, Y., and D.C. Chan. 2007. Structural basis for recruitment of mitochondrial fission complexes by Fis1. *Proc. Natl. Acad. Sci. USA.* 104:18526–18530. doi:10.1073/pnas.0706441104